Université de Montréal

Study of the Diffusion in Polymer Solutions and Hydrogels

by NMR Spectroscopy and NMR Imaging

par

WANG Yu Juan

Département de chimie

Faculté des arts et des sciences

Mémoire de Maîtrise présenté à la Faculté des études supérieures en vue de

l'obtention du grade de maîtrise en chimie

Novembre 2010

Université de Montréal

Faculté des études supérieures

Ce mémoire intitulé

Study of the Diffusion in Polymer Solutions and Hydrogels by NMR Spectroscopy and NMR Imaging

présenté par

WANG Yu Juan

a été évalué par un jury composé des personnes suivantes :

Prof. Michel Lafleur
président-rapporteur

Prof. Julian X. Zhu
directeur de recherche

Prof. Françoise Winnik
membre du jury

Mémoire accepté le :

Résumé

Afin d'étudier la diffusion et la libération de molécules de tailles inférieures dans un gel polymère, les coefficients d'auto-diffusion d'une série de polymères en étoile avec un noyau d'acide cholique et quatre branches de poly(éthylène glycol) (PEG) ont été déterminés par spectroscopie RMN à gradient de champ pulsé dans des solutions aqueuses et des gels de poly(alcool vinylique). Les coefficients de diffusion obtenus ont été comparés avec ceux des PEGs linéaires et dendritiques pour étudier l'effet de l'architecture des polymères. Les polymères en étoile amphiphiles ont des profils de diffusion en fonction de la concentration similaires à leurs homologues linéaires dans le régime dilué. Ils diffusent plus lentement dans le régime semi-dilué en raison de leur noyau hydrophobe. Leurs conformations en solution ont été étudiées par des mesures de temps de relaxation spin-réseau T_1 du noyau et des branches.

L'imagerie RMN a été utilisée pour étudier le gonflement des comprimés polymères et la diffusion dans la matrice polymère. Les comprimés étaient constitués d'amidon à haute teneur en amylose et chargés avec de l'acétaminophène (de 10 à 40% en poids). Le gonflement des comprimés, ainsi que l'absorption et la diffusion de l'eau, augmentent avec la teneur en médicament, tandis que le pourcentage de libération du médicament est similaire pour tous les comprimés.

Le gonflement *in vitro* des comprimés d'un complexe polyélectrolyte à base d'amidon carboxyméthylé et de chitosane a également été étudié par imagerie RMN. Ces comprimés sont sensibles au pH : ils gonflent beaucoup plus dans les milieux acides que dans les milieux neutres en raison de la dissociation des deux composants et de la protonation des chaînes du chitosane. La comparaison des résultats avec ceux d'amidon à haute teneur en amylose indique que les deux matrices ont des gonflements et des profils de libération du médicament semblables dans les milieux neutres, alors que les comprimés complexes gonflent plus dans les milieux acides en raison de la dissociation du chitosane et de l'amidon.

Mots-clés: RMN à gradient de champ pulsé, Imagerie RMN, Coefficients d'auto-diffusion, Polymère en étoile, Amidon à haute teneur en amylose, Chitosane

Abstract

In an effort to study the diffusion and release of small molecules in a polymeric system, the self-diffusion coefficients of a series of star polymers with a cholic acid core bearing four poly(ethylene glycol) (PEG) arms in aqueous solutions and gels of poly(vinyl alcohol) were determined by pulsed gradient spin-echo NMR techniques. The results have been compared with those of linear and dendritic PEGs to elucidate the effect of the architecture of the polymers. The amphiphilic star polymers show similar concentration-dependent diffusion behaviors in the dilute regime to their linear homologues. They diffuse more slowly in the semi-dilute regime than the linear PEGs due to the presence of the hydrophobic core. The conformation of the star polymers in the solutions was studied by measuring the T_1 values of the core and the arms of the diffusants.

NMR imaging was used to study the swelling of polymeric tablets and diffusion in the polymer matrix. The tablets investigated were made of cross-linked high amylose starch (CHAS) and loaded with acetaminophen (10, 20 and 40 wt%). The swelling, water uptake and diffusion in the CHAS network are faster at higher drug loading levels, while the drug release rates are similar among all the tablets.

The *in vitro* swelling of the tablets made of a polyelectrolyte complex based on chitosan and carboxymethylated starch has also been studied by NMR imaging. These tablets showed pH-sensitive behavior. They swelled much more in acidic media than in neutral media due to dissociation of the two components and the protonation of the amino groups in the chitosan residues. The comparison of the results with those obtained with the CHAS tablets indicates that the two matrices have similar swelling and drug release profile in neutral media, while the complex tablets showed a greater extent of swelling in acidic media due the dissociation of the chitosan from the complex.

Keywords: Pulsed gradient NMR spectroscopy, NMR imaging, Self-diffusion coefficients, Star polymer, High amylose starch, Chitosan.

Table of Contents

List of Figures

List of Tables

List of Symbols and Abbreviations

APAP	Acetaminophen
CAC	Critical aggregation concentration
CHAS	Cross-linked high amylose starch
CMS	Carboxymethyl starch
CMT	X-ray computed microtomography
CP-MAS	Cross-polarization magic angle spinning
δ	Length of a gradient pulse
Δ	Time interval between the two gradient pulses (diffusion time)
D	Self-diffusion coefficient
D_0	Initial diffusion coefficient of water
	Self-diffusion coefficient in pure water
DMF	N,N-dimethylformamide
FT-IR	Fourier transform infrared spectroscopy
γ	Gyromagnetic ratio of ^{1}H
G	Gradient strength
HPMC	Hydroxypropyl methylcellulose
M_n	Number average molecular weight
NMR	Nuclear magnetic resonance
NMRI	NMR imaging
PDI	Polydispersity index
PEG	Poly(ethylene glycol)
PEO	Poly(ethylene oxide)
PGSE	Pulsed-gradient spin-echo
pK_a	Logarithmic acid dissociation constant
PPI(TEG)$_n$	Poly(propylene imine) dendrimers bearing triethylenoxy

	methyl ether
PVA	Poly(vinyl alcohol)
R^2	Coefficients of determination
R_H	Hydrodynamic radius
SEM	Scanning electron microscopy
SEC	Size exclusion chromatography
SEC-LS	SEC coupled with a light scattering detector
SEC-RI	SEC coupled with a refractive index detector
SGF	Simulated gastric fluid
SIF	Simulated intestinal fluid
T_1	Longitudinal relaxation time
T_2	Transverse relaxation time
T_g	Glass-transition temperature
TE	Echo time
TR	Repetition time
USFDA	US Food and Drug Administration

Acknowledgements

I would like to thank all the people who supported, helped and inspired me during my study at the Université de Montréal.

First of all, I would like to thank my supervisor, Prof. Julian. X. Zhu, for his guidance through my study and research, for his enthusiasm, inspiration, and immense knowledge. He has also provided good teaching on how to make presentations and write papers, which will greatly benefit my future career.

I would like to thank Dr. Cédric Malveau for his training in NMR spectroscopy and valuable discussions. It is a great pleasure to work with him. He has made the NMR experiments very interesting and inspiring.

I am grateful to Prof. Mircea A. Mateescu and Mr. Elias Assaad at the Univesity of Québec at Montréal for their generous help with tablet preparation, dissolution tests and constructive discussions.

Mr. Sylvain Essiembre and Mr. Pierre Ménard-tremblay provided trainings on the instruments in the group and the maintenance of the instruments used for the characterization of polymers.

I am indebted to all members in our research group for providing a stimulating and fun environment in which to learn and grow.

Last but not least, I would like to thank my parents for their unflagging love and support throughout my life.

1. Introduction

Polymers have been widely used as excipients in the field of drug delivery. The pharmaceutical polymers provide the researchers with a wide choice of physical and chemical characteristics such as different molecular weight and possibility of copolymerisation, modification or blending with other polymers.[1] They include both natural polymers (such as starch, cellulose, chitosan, and pectin) and synthetic polymers (such as polyanhydrides, polyesters, polyacrylic acids, poly(methyl methacrylates), and polyurethanes). The wide range of physicochemical properties may be utilised to improve the clinical use, manufacturing, and stability of dosage forms.[1] More specifically, polymers have been used as binders, flow-controlling agents, and coatings in the conventional solid and liquid dosage forms. They are also essential parts to modify release characteristics in sustained drug release formulations.[2-4]

Drug dosage forms can be oral, inhalational, parenteral, topical, or suppository. Each of the forms has advantages and disadvantages. Different medical conditions or different drugs warrant different routes of administration. Around 84% of the 50 most-sold drug products in the United States and European markets are administered orally.[5] Once swallowed, with an adequate volume of water, a tablet will leave the oral cavity and rapidly pass along the esophagus into the stomach, where disintegration of the tablet might occur within minutes in the case of immediate-release dosage forms. The released drug will then dissolve in the gastrointestinal fluids, and the drug solution will pass directly into the small intestine, the optimal site for the absorption of most drugs into the systemic circulation. Drug absorption is normally completed in the small intestine, although on some occasions drug enters the large intestine where absorption of certain drugs is possible.[2]

However, some drugs may irritate the stomach or degrade at a pH between 2 or 3. It is advantageous to protect such drugs during passage into the small intestine. Colon delivery becomes increasingly important due to the increasing demand of oral administration of proteins and other macromolecules, such as insulin and heparin.[6] In order to minimize the exposure to proteolytic enzymes, enteric coating and controlled release are normally used to keep the drugs intact before they reach the target site of absorption.

In addition to providing the protection to the drug before reaching the absorption site, a controlled delivery can also maintain a prolonged therapeutic effect at a reduced dosing frequency.

A dosage form generally consists of one or more active ingredients together with a varying number of excipients added to facilitate the preparation and administration, promote the consistent release and bioavailability of the drug, and protect it from degradation.[7] According to their functions, excipients could be glidants, binders, diluents, and disintegrants. For example, an aminophylline table comprises aminophylline, corn starch, polyvinylpyrrolidone, magnesium stearate, hydrated magnesium silicate, and water.

Hydrogels are hydrophilic polymers commonly used as sustained release agents in pharmaceutical formulations because of their ability to form a gel network upon swelling, which entraps the drug and acts as a barrier to its release to the surrounding medium.

1.1. Polysaccharides as Drug Delivery Excipients

Polysaccharides are polymeric carbohydrate structures with repeating units joined together by glycosidic bonds. These structures are often linear, but may contain various degrees of branching. Polysaccharides are the most abundant natural polymers that exist in algae (e.g., alginate, carrageenan), plants (e.g., starch, cellulose, pectin, guar gum), microbes (e.g., dextran, xanthan gum), and animals (e.g., chitosan, chondroitin). Polysaccharides are highly stable, non-toxic, hydrophilic, degradable, and bioadhesive (adhesion to mucus gel). All of these properties are highly desirable for drug excipients. The pharmaceutical applications of polysaccharides have drawn much interest due to their proved ability to control drug release. The number of available polymers has substantially increased, leading to a wider range of applications.

Polysaccharides can be divided into three categories according to the functional groups attached to the glucose rings: anionic, cationic, and non-ionic polysaccharides. Starch and cellulose are non-ionic; chitosan is cationic due to the presence of $-NH_2$ groups; pectin, alginate, carrageenan are anionic due to the presence of $-COOH$ or SO_3^- groups. Non-ionic pharmaceutical polymer matrices exhibit pH-independent drug release profiles while ionic matrices show interesting pH-sensitive swelling behaviors, which is of great significance for

designing controlled release systems and cancer drug delivery due to the pH gradients in gastrointestinal tract from stomach to colon and across tumor cell compartments.[8, 9]

1.1.1. Starch

Starch is the safest carbohydrate. It consists of two types of molecules: the linear and helical amylose (20 – 25 wt%) and the highly branched amylopectin (75 – 80 wt%) (Figure 1.1). Amylose has a molecular weight approximately between 40,000 and 340,000, while amylopectin has a much higher molecular weight which may reach 80,000,000.
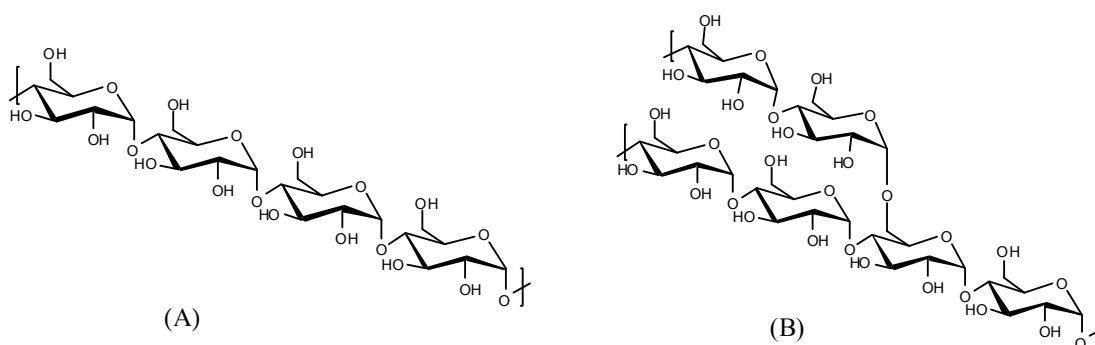
Figure 1.1. The chemical structures of (A) amylose and (B) amylopectin.

Starch is widely used as glidant, diluent, disintegrant and binder for tablets. It is generally recognized that drug release is strongly influenced by the starch origin and its degree of cross-linking in the tablet.[7, 10-12] The degree of cross-linking is directly related to the capacity of the starch to undergo a transition from V- to B-type double helix arrangement upon hydration, which is very important in controlling water transport and drug release rate.[13, 14]

The presence of –OH group at positions C2, C3, C6 of glucose allows for various modifications of amylose and amylopectin. Carboxymethyl starch has been studied for its gastroprotection capacity as it has a pK_a around 4.2. In acidic medium, carboxylic groups are protonated, giving a compact shape of the tablets.[15, 16] In the absence of cross-linking, drug release from monolithic tablets made of carboxymethyl starch is controlled by a combination of tablet erosion and diffusion of the drug from the swollen matrix.[15, 17, 18]

Both starch and sodium carboxymethyl starch have been approved by US Food and Drug

Administration (USFDA) for use as inactive ingredients in oral tablets and capsules.[19]

1.1.2. Cellulose

Cellulose is the skeletal substance of all vegetable tissues and the most abundant polymer on earth. It consists of a linear chain of several hundred to over ten thousand D-glucose units which are β-1,4 linked (Figure 1.2 A). Every other glucose in cellulose is flipped over due to the β-1,4 linkages, which promotes intrachain and interchain hydrogen bonds, as well as van der Waals interactions. These interactions make cellulose linear and highly crystalline.[7] Cellulose is insoluble in water and in most of the common solvents; the poor solubility is attributed primarily to the strong hydrogen bonding. However, the solubility may be enhanced by substitutions and is highly dependent on the degree of substitution. The cellulose derivatives are mainly obtained by esterifications and etherifications at the hydroxyl groups of cellulose, yielding products such as sodium carboxymethyl cellulose and methyl cellulose, etc. Hydroxypropyl methylcellulose (HPMC) (Figure 1.2 B) is one of the most commonly used polymers to retard the release of water-soluble drugs.[20-23] Since the hydroxypropyl group is hydrophilic and methoxyl group is hydrophobic, the ratio of hydroxypropyl to methoxyl content affects the extent of polymer interaction with water. This property will in turn influence water mobility in a hydrated gel layer and drug release.[20, 24, 25] The viscosity of HPMC plays an important role regulating tablet swelling and drug release. Higher viscosity grades of HPMC normally lead to slower swelling and drug release due to the greater effect of chain entanglement associated with higher molecular weights.[26]

Many cellulose derivatives have been approved by USFDA for use as inactive ingredients in oral tablets and capsules. They include carboxymethyl cellulose, cellulose acetate, ethylcellulose, methyl hydroxyethyl cellulose, and HPMC, etc.[19]

R_1, R_2, R_3 = H, CH_3, or $CH_2CH(OH)CH_3$

(A)   (B)
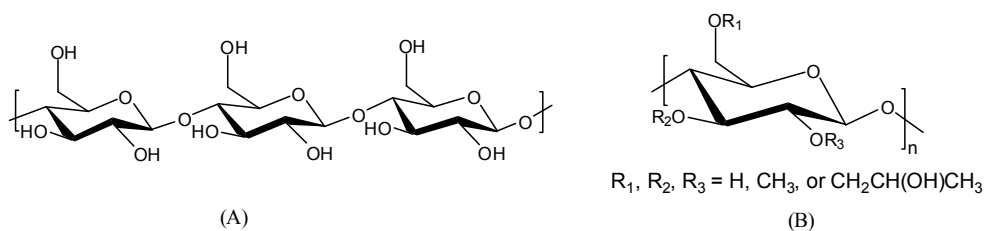
Figure 1.2. The chemical structures of (A) cellulose and (B) hydroxypropyl methyl cellulose (HPMC).

4

1.1.3. Chitosan

Chitosan has attracted research attention for decades.[27, 28] Chitosan is produced commercially by deacetylation of chitin, which is the structural element in the exoskeleton of crustaceans (crabs, shrimps, etc.). Chitosan is a linear cationic polysaccharide composed of randomly distributed β-1,4 linked D-glucosamine (deacetylated unit) and N-acetyl-D-glucosamine (Figure 1.3). Very interestingly, chitosan can prolong residence time in gastrointestinal tract through mucoadhesion, and enhance absorption by increasing permeability, which are major factors contributing to its widespread evaluation as a component of oral dosage forms. The pK_a value of chitosan is around 6.3. Chitosan is thus insoluble in water at neutral pH but soluble under slightly acidic conditions due to the protonation of the amine groups.[27] The pH sensitivity makes chitosan a unique polymer for oral drug delivery applications. However, the physicochemical properties of chitosan vary by its molecular weight, degree of deacetylation, the salt form, and charge density.
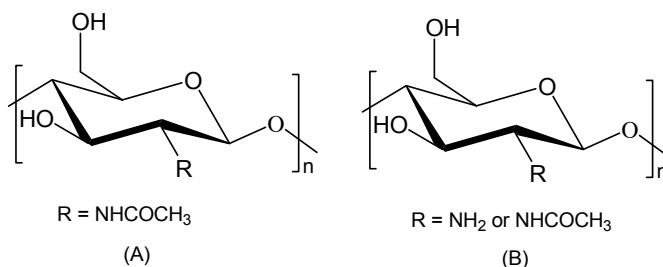
Figure 1.3. The chemical structures of (A) chitin and (B) chitosan.

Chitosan's amine groups and hydroxyl groups allow chemical derivatization by which the properties of this polymer can be modulated and adjusted to the intended application. This leads to a large variety of chitosan derivatives with different physical and biological properties, such as improved solubility and permeation enhancement.

To date, neither chitosan nor its derivatives has been approved by USFDA for use as inactive ingredients in oral drug dosage forms due to safety and tolerability concerns. Chitosan might cause mineral and vitamin depletion in the GIT.

To summarize, polysaccharides are biocompatible, biodegradable, mucoadhesive, and chemically versatile. The physicochemical properties and the drug delivery performances of

polysaccharides are influenced by factors such as ratio of components (amylose/amylopection ratio for starch, deacetylation degree of chitosan), molecular weight and viscosity, substitution degree, interaction between drug and matrix, cross-linking degree, and charge density, etc. The desirable pharmacokinetics may be tailored by functionalizations of the suitable polysaccharides. In the expanding field of controlled drug delivery, pharmaceutical polymers based on polysaccharides are playing an increasingly important role.

Other polysaccharides of pharmaceutical interest are presented in Appendix I for reference.

1.2. Drug Release Kinetics

Nearly all of the oral extended-release dosage forms fall into one of the following two technologies: matrix (monolithic) systems which consist of a rate-controlling polymer matrix through which the drug is dissolved or dispersed, and reservoir (coated) systems where drug-containing core is enclosed within a polymer coating.[20] A matrix tablet is the simplest and the most cost-effective method to fabricate an extended-release dosage form.

The mechanism of drug release from hydrophilic matrix tablets is based on diffusion of the drug and erosion of the outer hydrated polymer on the surface of the matrix.[20] Typically, when the matrix tablet is exposed to gastrointestinal fluids, the surface of the tablet is wetted and a gel layer formed around the matrix, which acts as a diffusing barrier to drug release. During the process, the polymer matrix undergoes a transition from the glassy to rubbery state. This leads to the relaxation of the matrix which also contributes to the mechanism of drug release. In the case of a highly soluble drug, an initial burst release occurs due to the presence of the drug on the surface of the matrix tablet. The gel layer (rubbery state) grows with time as more water permeates into the matrix, along with the shrinkage of the glassy core.

If the matrix is not cross-linked, as the outer layer becomes fully hydrated, the polymer chains become completely relaxed and can no longer maintain the integrity of the gel layer, thereby leading to disentanglement and erosion of the surface of the matrix. Water continues to penetrate towards the core of the tablet through the gel layer until it has been completely eroded.[20]

Only slight erosion occurs if the matrix is cross-linked. The tablet reaches its maximum

swelling after immersion in the media for a few hours, well before the whole tablet becomes fully hydrated. But the diffusing rates of the water towards the core and the drug out of the gel still increase until the processes reach equilibrium. The duration varies remarkably with the polymer matrix from 2-3 hours to days.

Drug solubility is an important factor determining the mechanism of drug release from hydrophilic matrix. Soluble drugs can be released by a combination of diffusion and erosion mechanisms whereas erosion is the predominant mechanism for insoluble drugs.[20, 29] The insoluble drug may dissolve slowly and have slow diffusion through the gel layer of the hydrophilic matrix. Therefore, the drug is released through the erosion of the surface of the hydrated matrix. For drugs with very high solubility, the drug dissolves within the gel layer and diffuses out into the media. Take HPMC tablets as an example, the drug release rate is controlled mainly by diffusion and erosion (or polymer dissolution) for soluble and insoluble drug, respectively.[26]

The diffusion in polymers can be divided into three categories depending on the rates of diffusion and relaxation. If the rate of diffusion is much lower than that of relaxation, the diffusion is called Case I or Fickian diffusion. In Case II, diffusion is much more rapid than the relaxation processes. Non-Fickian or anomalous diffusion occurs when the diffusion and relaxation rates are comparable.[30] Glassy polymers generally exhibit non-Fickian behavior while the diffusion in rubber polymers is Fickian because rubber polymers respond very rapidly to changes.[30]

A large number of mathematical models have been developed to describe drug release profiles from matrix systems.[20, 22, 31-33] The simplest yet most widely used model is the one derived by Korsmeyer et al.[34]:

$$M_t / M_\infty = k \cdot t^n \tag{1.1}$$

where M_t / M_∞ is the fraction of drug release, k is the diffusion rate constant, t is the release time and n is the exponent indicative of the mechanism of drug release. If a tablet is analogous to a slab, the exponent n is 1.0 or 0.5, the drug release mechanism follows zero-order release kinetics (also termed as Case II transport) or Fickian diffusion (Case I transport), respectively.[35] Values of n between 0.5 and 1 indicate the contribution of both the diffusion process as well as polymer relaxation in controlling the release kinetics (non-Fickian, anomalous or first-order release). For cylindrical tablets, these values are 0.45, 0.45

$< n < 0.89$ and 0.89 for Fickian, anomalous or Case II transport, respectively.[22] Drug release profiles from HPMC hydrophilic matrices are generally first-order for highly soluble drugs or zero-order for practically insoluble drugs, with the release exponent n ranging from 0.5 to 0.8.[20] The anomalous release is owing to the contribution of a mechanism other than diffusion of drug transport.[36]

More complex mechanistic theories that consider diffusion, swelling and dissolution processes simultaneously have been developed.[22] The choice of the appropriate mathematical model strongly depends on the desired predictive ability.

1.3. The Characterization of Polymer Matrices

The polymer matrix and the resultant tablets have been studied by various techniques, such as optical imaging,[12, 26, 37-39] mechanical method,[40] Fourier transform infrared spectroscopy (FT-IR),[11, 41] X-ray diffraction,[11, 41] X-ray computed microtomography (CMT),[42] scanning electron microscopy (SEM),[40, 42] cross-polarization magic angle spinning (CP-MAS) nuclear magnetic resonance (NMR) spectroscopy,[14, 43, 44] and NMR imaging.[45-50] Gravimetric experiments and dissolution tests are also widely used in the aim to study the drug release mechanism.

1.3.1. XRD and FT-IR Studies

The drug release rate of the tablets based on cross-linked high amylose starch (CHAS) was studied as a function of cross-linking degree, which showed that sustained release up to 20 h was achieved at a low cross-linking degree of 6% (the weight ratio of epichlorohydrin to high amylose starch). The CHAS tablets of higher cross-linking degree up to 20% showed a sharp decrease in the release time. Typically, a tetrafunctional polymer network would be created by increasing the degree of cross-linking, leading to a reduced swelling capacity. However, CHAS yielded a nonlinear response for swelling capacity and drug release.[51] X-ray diffraction studies suggested that the increase in cross-linking degree induces a transition of amylose from B-type (double helix) to a predominant V-type (single helix) and a loss in crystallinity. A high cross-linking degree also limited chain flexibility. Another consequence was that fewer chains were stabilized by interchain hydrogen-bonding and thus more

hydroxyl groups were available for dynamic exchange with free water, which facilitates hydration of the CHAS power, as reflected by the intensity of FT-IR water deformation vibration mode.[41] The conformation studies suggested that an optimized crystalline/amorphous ratio is responsible for tablet integrity during swelling, water penetration, and drug release of the CHAS-based monolithic dosage forms.[11]

1.3.2. SEM and CMT Studies

The SEM and CMT experiments demonstrated the skin-core structure of the CHAS tablets as a result of interaction with water and reorganization.[42] The core is surrounded by the skin consisting of two concentric layers, an inner porous membrane and an outer very dense membrane, which acts as pseudo-crosslinks and retain the integrity of the tablets.

The gravimetric method can be used to record water uptake of drug tablets. At appropriate time intervals, each tablet is removed from water and weighed. The water uptake data can be used to determine water diffusion mechanism. For example, the dynamic swelling and equilibrium swelling of poly(2-hydroxyethyl methacrylate-*co*-methacrylic acid) (poly(HEMA-*co*-MAA)) in buffer of different pH values were studied gravimetrically.[52] The mechanism of water diffusion in the gel became more anomalous as the pH of the swelling medium increased and as the ionic strength decreased at a constant $pH \geq pK_a$. The mechanism of water diffusion was Fickian and independent of ionic strength at a pH lower than the pK_a. The anionic polymeric networks ionized as the pH of the medium rose above the pK_a of that ionizable moiety. Increasing ionization at higher pH might affect the relative magnitude of diffusion and relaxation times. The reason is that the electrostatic repulsion between adjacent ionized carboxylate groups led to chain expansion, which in turn affected polymer chain relaxation. Despite the easy access, the gravimetric method has a disadvantage that the tablet transfer process and the ex-situ method would inevitably affect the swelling process and alter the fragile outer region of the gel, to the detriment of accuracy.

1.3.3. Dissolution Studies

Dissolution test is the only way to measure the rate of *in vitro* drug release as a function of time. Dissolution tests are commonly conducted according to the procedure now rigorously

and comprehensively defined in US Pharmacopeia. The objective of the dissolution test is to establish dissolution mechanism. In general, analytical methods used for quantifying drug release in dissolution tests can be classified into four categories: spectrophotometric, chromatographic, mass spectrometric, and potentiometric. Direct UV-vis spectrophotometric determination is most widely used for drug containing chromophores. The drug release profile is then used to determine whether the drug release is controlled by diffusion or by polymer relaxation mechanism.

A dissolution study was done to follow the behavior of CHAS derivatized with cationic (carboxymethyl), anionic (aminoalkyl) groups and less polar group (acetate) to study their release control properties and interactions with charged drugs (acetylsalicylic acid and metformin) and an uncharged drug (acetaminophen).[53] Ionic interactions retarded drug release effectively, the effect being more significant at high drug loading in the case of drugs of high solubility (such as metformin).

1.3.4. Optical Imaging

Optical imaging has been used to track the penetration of water into the tablets.[12, 26, 37-39] This method offers ease of manipulation with relatively low instrument cost. The gel layer normally appears as a bright ring and the dry core as a dark part due to the scattering of light by the hydrated polymer.[37] In digital image processing, the image is converted into a discrete number of points called pixels, which are assigned a numeric location and grey level value. The intensity of the signal was related to the water content in the tablets, the method is therefore not only used to monitor the tablet swelling, but also to characterize the moving front and the solvent concentration gradient. Optical imaging also demonstrated that the equilibrium swelling state was attained much after the solvent penetration fronts had met.[12] On the basis of the empirical relationship between scattered light intensity and HPMC concentration, the apparent gel region of a swelling HPMC tablet can be defined with respect to polymer concentration. The polymer concentration within the gel layer of HPMC tablets is around 5-50%.[37] As a matter of fact, the solvent penetration front goes slightly deeper than the apparent gel front. A very small portion of the gel region of higher polymer concentration is beyond the detection limit of optical imaging due to the opacity.

1.3.5. NMR Imaging Studies

NMR imaging (NMRI) has been used to study the matrix systems for more than a decade as NMRI can provide cross-sectional images from inside solid materials.[24, 39, 46-50, 54-63] Contrary to this, optical imaging can only observe the surface and the averaged diffraction signal of a tablet. NMRI uses magnetic field gradients to encode the NMR signal with spatial information. The amplitude of the signal indicates the water concentration at a particular position within the sample. The noninvasive and nondestructive nature of NMRI is especially advantageous for tracking the water penetration and the swelling of the matrix of the tablets in terms of both the development of the gel layer and the dimensional change of the core. Quantitative information can be obtained regarding the kinetics of the diffusion process and the polymer or drug concentration gradient upon hydration exclusively by NMRI rather than optical imaging.[12] A number of investigations[47, 49, 55, 56, 64, 65] aimed at characterizing the formation of the gel layer and determining how its properties influence drug release. Normally the images of the dimensional changes in the gel layer and the core are monitored and solvent concentration profiles (proton density profiles) are extracted from the images. NMRI can also be used to monitor the distribution of drug inside the tablets. For example, ^{19}F NMRI was chosen to measure triflupromazine–HCl and 5-fluorouracil concentration in HPMC-based tablets.[29]

Diffusion-weighted NMR imaging experiments are essential to studying the mobility of water inside the gel layer and determine the spatial distribution of self-diffusion coefficient of water. Such kind of studies showed that there was a water mobility gradient across the gel layer of HPMC and poly(vinyl alcohol) (PVA) matrices and the limited mobility of polymer chains near the glassy region hindered solvent transport.[24] From the outer gel to the glassy core, the self-diffusion coefficient of water decreases from that of free water (2×10^{-9} m^2/s at 25°C) to zero.[24]

1.3.6. Relaxation Time Studies

T_2 (transverse relaxation time) measurement of tablets is an interesting method to deduce the polymer concentration of hydrated layer of the swollen tablets.[45] Firstly, the dependence of the ^{1}H T_2 values on the HPMC weight fraction was obtained by measuring the relaxation times of equilibrated mixtures of HPMC solution of known concentrations. HPMC weight

percentages were then calculated from T_2 values with the determined calibration. At the same time, the percentages of the water bound to polymer and the free water were obtained.

1.4. Diffusion in Polymer-Water-Diffusant Systems

The diffusion of small molecules to macromolecules in polymer solutions and gels has attracted increasing research interest in the past decade. A particular important application involves the hydrogels as controlled release carriers of drugs. The effects of polymer concentration, size, and shape of the diffusant, temperature, and specific interactions within the polymer matrix are important in determining the diffusion properties in a polymer system. Our group has extensively studied the self-diffusion of small and large molecules in polymer-water-diffusant systems by pulsed-gradient spin-echo (PGSE) NMR spectroscopy.[66-73]

The diffusants having been studied included water, methanol, *tert*-butanol, formamide, acetic acid, trimethylamine, tetramethylammonium cation, oligo- and poly(ethylene glycol) of increasing molecular weight from 62 to 10,000,[66-69] a series of end-capped ethylene glycol and oligo(ethylene glycol),[70] poly(propyleneimine) dendrimers (generations 2, 4, and 5),[71] hyperbranched polyglycidols,[72] and carboxylated dendrimers.[73]

The matrices are mainly poly(vinyl alcohol) (PVA).[66-73] Besides, hydroxypropyl methyl cellulose (HPMC),[69] poly(N,N-diethylacrylamide) (PNNDEA),[69] poly(N-isopropylacrylamide) (PNIPA),[69] and poly(allyl amine) (PAAm)[73] were also used to study the effects of different matrices and ionic interactions between the diffusants and the polymer matrices.

1.4.1. Molecular Size of the Diffusant

It was found that at a given polymer concentration the size of the diffusant has the most significant effect on its diffusion in the absence of strong interactions between the diffusants and the polymer network.[66-72]

1.4.2. Concentration of the Polymer

The self-diffusion coefficient of diffusants ranging from small molecules to macromolecules in PVA solutions and gels decreased with increasing PVA concentration (from 0 to 0.38 g/mL).[66-73]

1.4.3. Molecular Weight and Hydrolysis Degree of the Polymer

The diffusion of both small molecules and linear poly(ethylene glycol)s (PEGs) did not vary significantly with the molecular weight (50,000 and 115,000) of the PVA matrix, and only a small variation was observed with the degree of hydrolysis of the PVA (87% and 99%).[66]

1.4.4. Geometry of the Diffusant

The molecular geometry of the diffusant plays an important role in the diffusion process, as reflected by a study of a series of end-capped ethylene glycol and oligo(ethylene glycol)s in PVA aqueous solutions and gels.[70] The end groups included both flexible groups (methyl, ethyl, hexyl) and rigid groups (*tert*-butyl and aromatic groups). The results showed that the methyl groups reduced or prevented the binding of ethylene glycol to PVA.[70] Diffusants with a bulkier end group (such as *tert*-butyl group) diffused less rapidly than those with a smaller linear end group even though the molecular weights of the molecular are comparable.[70]

The dendritic polymers, poly(propyleneimine) dendrimers with hydrophilic triethylenoxy methyl ether terminal groups diffused faster in PVA aqueous solutions and gels than the linear PEGs when the molecular weights were similar.[71] Hyperbranched polyglycidols of molecular weights from 300 to 2000 were also studied.[72] For diffusants of similar molecular weight and without specific interactions, the activation energy increased from the dendrimers to hyperbranched polymers and then to linear polymers.[72]

1.4.5. Effect of Temperature

The studies on the effect of temperature on the diffusion of oligo- and poly(ethylene glycol)s showed that the self-diffusion coefficients increased with increasing temperature.[67, 68, 71, 73]

1.4.6. Interaction Between the Diffusants and the Polymers

The study of the diffusion of small molecules with different functional groups (alcohol, amine, ammonium salt, amide, and acid) in PVA solutions and gels showed that the interactions had little impact on the diffusion behaviour because the diffusion was primarily influenced by the size of the diffusant.[66]

The ionic interaction between the carboxylated dendritic diffusants and the cationic poly(allyl amine) network significantly reduced the diffusion rate of the diffusant. The self-diffusion coefficients were an order of magnitude lower than those in PVA and the values were more widely distributed.[73]

1.4.7. Various Polymer Matrices

The effect of the polymer matrices on the self-diffusion of PEG with a molecular weight 600 was studied for different ternary polymer-water-PEG systems (PVA, HPMC, PNNDEA, and PNIPA).[69] The diffusion in hydrophilic polymers was mostly affected by formation of the hydrogen bonds between the solute and the polymer matrix.

Several pertinent physical models of diffusion were evaluated and the physical significance of the parameters were analyzed as well.[67] These models were based on the obstruction effect, the free volume effect, or hydrodynamic interactions. The difficulties in their applications include failure to describe large probes, lack of knowledge of some parameters that are not readily available, and lack of physical significance of the parameters.[67-69] Our group proposed a model suitable for both small and large diffusants in dilute and concentrated polymer systems.[74] This model has been validated by a number of diffusants in the polymer-water-diffusant ternary systems, including oligo- and poly(ethylene glycol)s,[67, 68, 70] dendrimers,[71, 73] hyperbranched polyglycidols[72] in PVA, water and PEG[69] in PVA, HPMC, PNNDEA, and PNIPA. In all the cases, the model successfully described the effects of polymer concentration, temperature, and molecular size of the diffusants.

1.5. Water Diffusion in CHAS Tablets

The CHAS powder has been prepared according to US patents.[75, 76] The starch of a high

content of amylose was chosen because it yielded a stronger gel.[51] Firstly, high-amylose starch was activated by heating in sodium hydroxide solution. Phosphorous oxychloride was used as the cross-linking agent along with propylene oxide added to further functionalize amylose and amylopectin molecules. Covalent cross-links and hydroxypropyl side chains of the final product allow greater stability by hindering retrogradation over time.[51] Retrogradation of starch is used to define the changes from amorphous state to a more ordered or crystalline state.

CHAS attracted attention due to its sustained drug release property as an excipient of oral drug dosage form. A membrane at the outer layer of CHAS tablets quickly formed upon hydration and the tablets could maintain the integrity in water for days. The absence of erosion and limited swelling allow for further explorations of the applications in drug delivery.[13]

CHAS tablets have been extensively studied by NMRI and a few other polymer characterization techniques by our group.[46-50, 55] The result obtained were summarized hereafter.

1.5.1. Swelling of CHAS Tablets

Similar to other tablets, when a CHAS tablet is immersed into water, water penetrates into the hydrophilic polymer matrix easily to form a hydrogel, leading to a steep water gradient. The formation of the membrane which acts as a barrier opposing water and drug transport was well characterized by NMRI.[42, 49] The glassy-rubbery transition is based on the lowering of the glass-transition temperature (T_g) of the polymer, which is controlled by the water concentration and depends on temperature and thermodynamic interactions of the polymer-water system.[36] The swelling of the CHAS tablets approaches its maximum at around 10 h at 37 °C but 60% of swelling can be achieved within the first 4 h.[48]

The swelling is anisotropic with the axial swelling being much more significant than the radial swelling for all the tablets of different sizes and within the temperature range from 25 to 60 °C.[46-48] The more pronounced axial swelling was related to the relief of the stresses induced during compaction of the matrix tablets.[77] However, the gel layer along both directions are similar in thickness.[39]

1.5.2. Effect of Temperature

Four temperatures (25, 37, 45, and 60 $^{\circ}$C) were employed to study the water diffusion and the swelling of the CHAS tablets.[46, 48] The tablets have a faster swelling with increasing temperature up to 60 $^{\circ}$C. The diffusion process is Fickian between 25 and 45 $^{\circ}$C and Case II at 60 $^{\circ}$C. The difference is caused by the different degrees of the transformation from V-type single helix polymorph to B-type double helices during water uptake.[47, 48] The double helical conformation acts as physical cross-links which in turn limits the swelling and thus is essential for sustained drug release, which is verified by CP-MAS ^{13}C NMR spectroscopy. The details of the transformation include the following steps with water penetrating into a tablet to act as a plasticizing agent. This plasticizing effect increases intermolecular space and thus allows greater mobility to starch molecules which rapidly start reorganizing into the thermodynamically most stable conformations: B-type double helices.[51]

1.5.3. Effect of the Tablet Size

The water uptake and the tablet swelling strongly depend on the size of the tablets.[47] The swelling rate is faster for the small tablet along both swelling directions due to its larger surface/volume ratio. In both cases, the decrease of the dry thickness is more rapid than that of the dry diameter with immersion time.

1.5.4. Effect of Drug Loading

The drug loading effect has been studied by comparing tablets loaded with 10 wt% soluble drugs (ciprofloxacin and acetaminophen) and tablets containing exclusively polymer matrix.[49] The extent of the swelling of the tablets was not noticeably influenced by a 10 wt% drug-loading, since the presence of drugs at this content did not interfere with the formation of double helices which limited the overall swelling of the CHAS tablets.[49] However, the presence of drug molecules caused a faster water uptake, as reflected by the higher diffusion coefficients of water.

1.6. Objectives of This Study

The objective of the study is to elucidate the effect of architecture of polymers, the level of drug loading, and the pH value and ionic strength of the environment on the diffusion of the diffusant and the swelling of the polymer matrices. A justification for these choices follows.

Every natural or synthetic polymer falls into one of the following categorized architectures: linear, graft, branched, cross-linked, star-shaped, and dendritic. The effect of shape of the diffusants has been preliminarily investigated by comparing the diffusion of linear, dendritic, and hyperbranched polymers in polymer aqueous solutions and gels.[71, 72] As a series of star-shaped polymers with four arms have been successfully synthesized in our group, a comparison among the polymers of different architectures becomes highly desirable.

Hydrophilic drugs have been believed to trigger water uptake and water diffusion into the polymer matrix, and thus it is challenging to yield a sustained release when the level of drug loading is high. The CHAS tablets loaded with only 10 wt% of drug have been studied up to now. It is important to measure the rate of water diffusion in the tablets with different drug loading levels and to correlate it with the swelling of the tablets and the rate of drug dissolution.

In the past, all the NMR Imaging studies of the CHAS tablets used only water as the medium. To study the swelling of the tablets and the solvent uptake in the physiological environment (for example, the media simulating the stomach and the small intestine fluids) is of significant importance. To understand the effect of pH on the drug release from a certain matrix is also highly desirable due to the different pH values in human's gastrointestinal tract. The pH value and ionic strength are expected to significantly affect the swelling of the polymer matrices containing ionic groups. A chitosan-based polyelectrolyte complex is an interesting material which shows pH-dependent association and dissociation among the ionic groups attached to the polymer chains. It should be compared with CHAS.

1.7. Scope of This Study

This thesis comprises of a series of studies leading to the development of a relationship between drug release kinetics and physicochemical properties of polymers such as the

diffusion coefficients of the polymer and water, liquid uptake, and kinetics of swelling of the matrices.

Chapter 2 focuses on the diffusion of a star polymer in aqueous solution and PVA gel studied by PGSE NMR spectroscopy. An amphiphilic star polymer is compared with linear polymers and dendrimers.

Chapter 3 presents the effect of drug loading on water uptake kinetics, swelling, drug release of CHAS tablets. The effect is studied by NMR imaging, drug dissolution experiments complementary to a quantitative measurement of diffusion coefficients in the hydrated tablets with acetaminophen loading up to 40 wt%.

Chapter 4 describes the effect of pH and ionic strength of the external media on the swelling of tablets made of a polyelectrolyte complex. The complex is formed between chitosan and sodium carboxymethyl starch (CMS).

The thesis concludes with a summary and suggestions for future work. Studies on the effect of polymer architecture, drug loading, and various media would be valuable for the development and optimization of biopolymer systems for drug delivery.

1.8. References

1.   Jones, D., *Pharmaceutical Applications of Polymers for Drug Delivery*. Rapra Technology Limited: Shropshire, UK, 2004; Vol. 15.

2.   Kendall, R. A.; Basit, A. W., The Role of Polymers in Solid Oral Dosage Forms. In *Polymer in Drug Delivery*, Uchegbu, I.; Schatzlein, A., Eds. CRC Press: Boca Raton, 2006.

3.   Alexander, C. *Expert Opin. Emerging Drugs* **2001,** 6, 345-363.

4.   Chaubal, M. V., Polymeric Excipients for Controlled Release Applications. In *Excipient Development for Pharmaceutical, Biotechnology, and Drug Delivery Systems*, Katdare, A.; Chaubal, M. V., Eds. Informa Healthcare USA, Inc. : New York, 2006.

5.   Abrahamsson, B.; Lennernäs, H., Application of the Biopharmaceutic Classification System Now and in the Future. In *Drug Bioavailability: Estimation of Solubility, Permeability, Absorption and Bioavailability*, Waterbeemd, H. v. d.; Lennernäs, H.; Artursson, P., Eds. Wiley-VCH: Weinheim, 2003.

6.   Goldberg, M.; Gomez-Orellana, I. *Nat. Rev. Drug Discov.* **2003,** 2, 289-295.

7.   Klein, S., Polysaccharides in Oral Drug Delivery –Recent Applications and Future Perspectives In *Polysaccharide Materials: Performance by Design*, Edgar, K. J.; Heinze, T.; Buchanan, C. M., Eds. ACS: 2009.

8.   Na, K.; Bae, Y. H., pH-Sensitive Polymers for Drug Delivery In *Polymeric Drug Delivery Systems*, Kwon, G. S., Ed. Taylor & Francis Group: Boca Raton, FL, 2005.

9.   Shen, Y.; Tang, H.; Radosz, M.; Kirk, E. V.; Murdoch, W. J., pH-Responsive Nanoparticles for Cancer Drug Delivery. In *Drug Delivery Systems*, Jain, K. K., Ed. Humana Press: Totowa, NJ, 2008.

10.   Onofre, F.; Wang, Y.-J.; Mauromoustakos, A. *Carbohydr. Polym.* **2009,** 76, 541-547

11.   Ispas-Szabo, P.; Ravenelle, F.; Hassan, I.; Preda, M.; Mateescu, M. A. *Carbohydr. Res.* **2000,** 323, 163-175.

12.   Moussa, I. S.; Cartilier, L. H. *J. Control. Release* **1996,** 42, 47-55.

13.   Lenaerts, V.; Moussa, I.; Dumoulin, Y.; Mebsout, F.; Chouinard, F.; Szabo, P.; Mateescu, M. A.; Cartilier, L.; Marchessault, R. *J. Control. Release* **1998,** 53, 225-234.

14.   Thérien-Aubin, H.; Janvier, F.; Baille, W. E.; Zhu, X. X.; Marchessault, R. H. *Carbohydr. Res.* **2007,** 342, 1525-1529.

15.   Massicotte, L. P.; Baille, W. E.; Mateescu, M. A. *Int. J. Pharm.* **2008,** 356, 212-223.

16.   Calinescu, C.; Mateescu, M. A. *Eur. J. Pharm. Biopharm.* **2008,** 70, 582-589.

17.   Sen, G.; Pal, S. *J. Appl. Polym. Sci.* **2009,** 114, 2798-2805.

18.   Brouillet, F.; Bataille, B.; Cartilier, L. *Int. J. Pharm.* **2008,** 356, 52-60.

19.   Inactive ingredients database. http://www.accessdata.fda.gov/scripts/cder/iig/index.cfm (April 3, 2010),

20.   Tiwari, S. B.; Rajabi-Siahboomi, A. R., Extended-Release Oral Drug Delivery Technologies: Monolithic Matrix Systems. In *Drug Delivery Systems*, Jain, K. K., Ed. Humana Press: Totowa, NJ 2008.

21.   Cao, Q. R.; Choi, Y. W.; Cui, J. H.; Lee, B. J. *J. Control. Release* **2005,** 108, 351-361.

22.   Siepmann, J.; Peppas, N. A. *Adv. Drug Deliver. Rev.* **2001,** 48, 139–157.

23.   Rowe, R. C.; Sheskey, P. J.; Quinn, M. E., *Handbook of Pharmaceutical Excipients*. 6th ed.; Pharmaceutical Press: London, 2009.

24.   Rajabi-Siahboomi, A. R.; Bowtell, R. W.; Mansfield, P.; Davies, M. C.; Melia, C. D. *Pharm. Res.* **1996,** 13, 376-380.

25. McCrystal, C. B.; Ford, J. L.; Rajabi-Siahboomi, A. R. *J. Pharm. Sci.* **1999,** 88, 797-801.

26. Pham, A. T.; Lee, P. I. *Pharm. Res.* **1994,** 11, 1379-1384.

27. Kumar, M. N. V. R.; Muzzarelli, R. A. A.; Muzzarelli, C.; Sashiwa, H.; Domb, A. J. *Chem. Rev.* **2004,** 104, 6017-6084.

28. Park, J. H.; Saravanakumar, G.; Kim, K.; Kwon, I. C. *Adv. Drug Deliver. Rev.* **2010,** 62, 28-41.

29. Fyfe, C. A.; Blazek-Welsh, A. I. *J. Control. Release* **2000,** 68, 313-333.

30. Crank, J., *The Mathematics of Diffusion*. 2nd ed.; Oxford University Press: Oxford, 1975.

31. Narasimhan, B. *Adv. Drug Deliver. Rev.* **2001,** 48, 195-210.

32. Siepmann, J.; Göpferich, A. *Adv. Drug Deliver. Rev.* **2001,** 48, 229-247.

33. Parker, R. S.; Doyle III, F. J. *Adv. Drug Deliver. Rev.* **2001,** 48, 211-228.

34. Korsmeyer, R. W.; Gurny, R.; Doelker, E.; Buri, P.; Peppas, N. A. *J. Pharm. Sci.* **1983,** 72, 1189–1191.

35. Bajwa, G. S.; Hoebler, K.; Sammon, C.; Timmins, P.; Melia, C. D. *J. Pharm. Sci.* **2006,** 95, 2145–2157.

36. Colombo, P.; Bettini, R.; Santi, P.; Peppas, N. A. *Pharm. Sci. Technol. To.* **2000,** 3, 198-204.

37. Gao, P.; Meury, R. H. *J. Pharm. Sci.* **1996,** 85, 725-731.

38. Bussemer, T.; Peppas, N. A.; Bodmeier, R. *Eur. J. Pharm. Biopharm.* **2003,** 56, 261-270.

39. Moussa, I. S.; Lenaerts, V.; Cartilier, L. H. *J. Control. Release* **1998,** 52, 63–70.

40. Ravenelle, F.; Marchessault, R. H.; Legare, A.; Buschmann, M. D. *Carbohydr. Polym.* **2002,** 47, 259-266.

41. Dumoulin, Y.; Alex, S.; Szabo, P.; Cartilier, L.; Mateescu, M. A. *Carbohydr. Polym.* **1998,** 37, 361-370.

42. Chauve, G.; Ravenelle, F.; Marchessault, R. H. *Carbohydrate Polymers* **2007,** 70, 61-67.

43. LeBail, P.; Morin, F. G.; Marchessault, R. H. *Int. J. Biol. Macromol.* **1999,** 26, 193-200.

44. Shiftan, D.; Ravenelle, F.; Mateescu, M. A.; Marchessault, R. H. *Starch-Starke* **2000,** 52, 186-195.

45. Fyfe, C. A.; Blazek, A. I. *Macromolecules* **1997,** 30, 6230-6237.

46. Baille, W. E.; Malveau, C.; Zhu, X. X.; Marchessault, R. H. *Biomacromolecules* **2002,** 3, 214-218.

47. Malveau, C.; Baille, W. E.; Zhu, X. X.; Marchessault, R. H. *Biomacromolecules* **2002,** 3, 1249-1254.

48. Thérien-Aubin, H.; Baille, W. E.; Zhu, X. X.; Marchessault, R. H. *Biomacromolecules* **2005,** 6, 3367-3372.

49. Thérien-Aubin, H.; Zhu, X. X.; Ravenelle, F.; Marchessault, R. H. *Biomacromolecules* **2008,** 9, 1248-1254.

50. Thérien-Aubin, H.; Zhu, X. X. *Carbohydr. Polym.* **2009,** 75, 369-379.

51. Ravenelle, F.; Rahmouni, M., Contramid: High-Amylose Starch for Controlled Drug Release. In *Polysaccharides for Drug Delivery and Pharmaceutical Applications*, Marchessault, R. H.; Ravenelle, F.; Zhu, X. X., Eds. American Chemical Society: Washington, DC, 2006; pp 79-104.

52. Khare, A. R.; Peppas, N. A. *Biomaterials* **1995,** 16, 559-567.

53. Mulhbacher, J.; Ispas-Szabo, P.; Lenaerts, V.; Mateescu, M. A. *J. Control. Release* **2001,** 76, 51-58.

54. Dahlberg, C.; Fureby, A.; Schuleit, M.; Dvinskikh, S. V.; Furo, I. *J. Control. Release* **2007,** 122, 199-205.

55. Thérien-Aubin, H.; Zhu, X. X., Water diffusion in drug delivery systems made of high-amylose starch as studied by NMR imaging. In *Polysaccharides For Drug Delivery And Pharmaceutical Applications*, Marchessault, R. H.; Ravenelle, F.; Zhu, X. X., Eds. American Chemical Society: Washington, D. C., 2006; pp 105-120.

56. Richardson, J. C.; Bowtell, R. W.; Mader, K.; Melia, C. D. *Adv. Drug Deliv. Rev.* **2005,** 57, 1191-1209.

57. Kowalczuk, J.; Tritt-Goc, J.; Pislewski, N. *Solid State Nucl. Magn. Reson.* **2004,** 25, 35-41.

58. Chowdhury, M. A.; Hill, D. J. T.; Whittaker, A. K.; Braden, M.; Patel, M. P. *Biomacromolecules* **2004,** 5, 1405-1411.

59. Chowdhury, M. A.; Hill, D. J. T.; Whittaker, A. K. *Biomacromolecules* **2004,** 5, 971-976.

60. Ghi, P. Y.; Hill, D. J. T.; Whittaker, A. K. *Biomacromolecules* **2001,** 2, 504-510.

61. Fahie, B. J.; Nangia, A.; Chopra, S. K.; Fyfe, C. A.; Grondey, H.; Blazek, A. *J. Control. Release* **1998,** 51, 179-184.

62. Hopkinson, I.; Jones, R. A. L.; Black, S.; Lane, D. M.; McDonald, P. J. *Carbohydr. Polym.* **1997,** 34, 39-47.

63. Rajabi-Siahboomi, A. R.; Bowtell, R. W.; Mansfield, P.; Henderson, A.; Davies, M. C.; Melia, C. D. *J. Control. Release* **1994,** 31, 121-128.

64. Baumgartner, S.; Lahajnar, G.; Sepe, A.; Kristl, J. *Eur. J. Pharm. Biopharm.* **2005,** 59, 299-306.

65. Kulinowski, P.; Dorozynski, P.; Jachowicz, R.; Weglarz, W. P. *J. Pharm. Biomed.* **2008,** 48, 685-693.

66. Petit, J.-M.; Zhu, X. X.; Macdonald, P. M. *Macromolecules* **1996,** 29, 70-76.

67. Masaro, L.; Zhu, X. X.; Macdonald, P. M. *Macromolecules* **1998,** 31, 3880-3885.

68. Masaro, L.; Zhu, X. X.; Macdonald, P. M. *J. Polym. Sci., Part B: Polym. Phys.* **1999,** 37, 2396-2403.

69. Masaro, L.; Ousalem, M.; Baille, W. E.; Lessard, D.; Zhu, X. X. *Macromolecules* **1999,** 32, 4375-4382.

70. Masaro, L.; Zhu, X. X. *Macromolecules* **1999,** 32, 5383-5390.

71. Baille, W. E.; Malveau, C.; Zhu, X. X.; Kim, Y. H.; Ford, W. T. *Macromolecules* **2003,** 36, 839-847.

72. Baille, W. E.; Zhu, X. X.; Fomine, S. *Macromolecules* **2004,** 37, 8569-8576.

73. Thérien-Aubin, H.; Zhu, X. X.; Moorefield, C. N.; Kotta, K.; Newkome, G. R. *Macromolecules* **2007,** 40, 3644-3649.

74. Petit, J.-M.; Roux, B.; Zhu, X. X.; Macdonald, P. M. *Macromolecules* **1996,** 29, 6031-6036.

75. Lenaerts, V.; Beck, R. H. F.; Van Bogaert, E.; Chouinard, F.; Hopcke, R.; Desevaux, C. Cross-linked high amylose starch for use in controlled-release pharmaceutical formulations and processes for its manufacture. U.S. Patent 6,607,748, August 19, 2003.

76. Mateescu, M. A.; Lenaerts, V.; Dumoulin, Y. Use of cross-linked amylose as a matrix for the slow release of biologically active compounds U. S. Patent 5,456,921, Oct.10, 1995.

77. Papadimitriou, E.; Buckton, G.; Efentakis, M. *Int. J. Pharm.* **1993,** 98, 57-62.

2. Effect of Molecular Architecture on the Self-Diffusion of Polymers in Aqueous Systems: A Comparison of Linear, Star, and Dendritic Poly(ethylene glycol)s[*]

2.1. Abstract

Star polymers with a hydrophobic cholane core and four poly(ethylene glycol) (PEG) arms, $CA(EG_n)_4$, have been synthesized by anionic polymerization. Pulsed-gradient spin-echo NMR spectroscopy was used to study the diffusion behavior of the star polymers, ranging from 1000 to 10,000 g/mol, in aqueous solutions and gels of poly(vinyl alcohol) (PVA) at 23°C. The star polymers have a lower self-diffusion coefficient than linear PEGs at equivalent hydrodynamic radius. In water alone, the star polymers and their linear homologues have a similar diffusion behavior in the dilute regime, as demonstrated by the similar concentration dependence of the self-diffusion coefficients. In the semidilute regime, the star polymers tend to aggregate due to their amphiphilic properties, resulting in lower self-diffusion coefficients than those of linear PEGs. ^1H NMR T_1 measurements at 10-70 °C revealed that the PEG arms of the star polymers are more mobile than the core, suggesting the star polymers in solution have a conformation similar to that of poly(propylene imine) dendrimers.

2.2. Introduction

The study of diffusion is of fundamental importance in describing macromolecular solution dynamics. The determination of diffusion coefficients of macromolecules in solutions or gels of polymer matrices is also important for applications such as controlled delivery of drugs, gel electrophoresis, permeation through membranes, plasticizers in plastic materials, and encapsulation of drugs and fragrances.[1-4] The diffusion behavior of a variety of oligomers and polymers, including linear poly(ethylene glycol) (PEG),[5-8] dendrimer,[9, 10] hyperbranched,[11-13] and star polymers[14-16] have been studied. The understanding of the dependence of the transport behaviors of the diffusants on their size and shape may help in the design of polymer systems with predictable properties.[17, 18] The shape of a macromolecule

may have a pronounced effect on its diffusion coefficient. For example, the rodlike protein tropomyosin (aspect ratio $R = 26$) and globular protein myoglobin (aspect ratio $R = 1.6$) exhibited similar behavior in agarose gels but markedly different diffusion in carrageenan gel,[19] since agarose gel has a mesh size about 6 times of that of carrageenan gel, in which the diffusion of stiff tropomyosin was hindered more significantly. In aqueous solutions of poly(vinyl alcohol) (PVA), a cyclic poly(ethylene oxide) (PEO) of a lower molecular weight ($M_n = 6\ 000$) was found to have almost the same self-diffusion coefficients as linear PEO of a higher molecular weight ($M_n = 10\ 000$).[20]
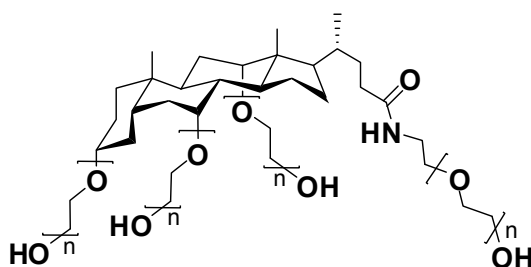
Figure 2.1. The chemical structure of the star polymers used in this study. They are prepared by anionic polymerization of ethylene oxide on a core of cholic acid.[21] Four PEG chains are attached and the chain length $n = 4, 6, 10, 17, 31, 39$, and 54.

Star polymers have attracted significant research interests due to their compact structures and unique physical properties.[22-24] Pulsed-gradient spin-echo (PGSE) NMR experiments have revealed that the molecular mobility of star-branched polyisoprenes in C_6F_5Cl and CCl_4 solutions depends largely on the weight fraction of the polymer, and only weakly on the number of the arms.[14] Similarly, no marked difference was observed between linear and three-armed polystyrenes and polybutadienes ($M_n = 3,000 - 1,000,000$) in CCl_4 solution from dilute to semidilute regime.[15] Although considerable research concerning the shape effect on both the static and dynamic parameters of polymer solutions has been conducted, very few general conclusions can be drawn. The factor of molecular shape is more difficult to address than the molecular size and the accumulation of results helps in the elucidation of such effects. We have previously compared the self-diffusion of linear PEGs and poly(propylene imine) dendrimers bearing triethylenoxy methyl ether as end groups (PPI(TEG)$_n$).[9] In this work, we used star polymers CA(EG$_n$)$_4$, newly made by attaching four PEG chains to a

24

cholane core (Figure 2.1) by anionic polymerization[21] and studied their diffusion behaviors using the PGSE NMR technique. The star polymers with bile acid cores were characterized in a previous study.[21] All three series of polymers, star polymers $CA(EG_n)_4$, linear PEGs, and poly(propylene imine) dendrimers, share the same repeat unit, ethylene glycol, while the cores of the star polymers (cholic acid) and dendrimers (poly(propylene imine)) add structural variants for the comparative studies. The self-diffusion coefficient measurements were performed in either binary solutions of the diffusants or ternary systems of PVA-water-diffusant.

2.3. Experimental

2.3.1. Materials

PVA (MW = 89,000 – 98,000, 99% hydrolyzed) and deuterium oxide (D_2O) were purchased from Sigma-Aldrich (Milwaukee, WI). All chemicals were used as received. The star polymers (Figure 2.1) were synthesized as reported previously.[21] The molecular weights of the star polymers measured by size exclusion chromatography (SEC), MALDI-TOF mass spectrometry, and NMR spectroscopy[21] are listed in Table 2.1 and all results show very low polydispersity indices (PDI = 1.02 ~ 1.05). The molecular weight were obtained both by SEC coupled with a refractive index detector (SEC-RI) calibrated with linear homologues and by SEC with a light scattering detector (SEC-LS). Both detection methods provided similar results, while the absolute molecular weights measured by SEC-LS are systematically 1.1 times of the values obtained by SEC-RI. It should be noted, however, that linear PEGs were used as the standards for SEC-RI. The molecular weights listed in the report are those obtained by SEC-RI unless otherwise specified. The refractive index increment, dn/dc, was measured with a series of 8 solution samples in the concentration range of 0.2 – 3.0 mg/mL for each polymer, using a refractive index detector from Wyatt. The molecular weights were determined by SEC equipped with a differential refractometer (Optilab) and a multiangle light scattering detector (DAWN EOS, wavelength 690 nm) in *N,N*-dimethylformamide (DMF) at a flow rate of 0.5 mL/min at 25 °C with a set of styragel columns (a TSK-gel α-M, particle size 13 μm, exclusion limit 1×10^7 Da for polystyrene in DMF, and a TSK-gel α-3000, particle size 7 μm, exclusion limit 1×10^5 Da for polystyrene in DMF) (Tosoh Biosep).

Samples were filtered through 0.2 μm membrane filters before injection (volume 100 μL). In the NMR studies, the ratio of the peak intensity of CH_2 of the PEG segment (3.6 ppm) to that of the CH_3 of the cholane core (0.6 ppm) is used for the calculation of molecular weight.

Table 2.1. The molecular weights of the star polymers CA(EG$_n$)$_4$ determined by SEC, MALDI-TOF mass spectrometry, and ^{1}H NMR spectroscopy

Samples [a]	SEC		MALDI-TOF		^{1}H NMR
	M_n	PDI	M_n	PDI	M_n
	(g/mol)		(g/mol)		(g/mol)
CA(EG$_4$)$_4$	1110	1.04	1360	1.03	1410
CA(EG$_6$)$_4$	1510	1.04	1810	1.03	2180
CA(EG$_{10}$)$_4$	2190	1.04	2430	1.03	3140
CA(EG$_{17}$)$_4$	3500	1.03	4230	1.03	5490
CA(EG$_{31}$)$_4$	5870	1.05	5980	1.03	8600
CA(EG$_{39}$)$_4$	7320	1.03	6860	1.02	11340
CA(EG$_{54}$)$_4$	9890	1.05			15450

[a] The degrees of polymerization (n) are calculated from M_n by SEC.

2.3.2. Sample Preparation

Samples for self-diffusion measurements were prepared following a method described previously.[6, 9] A D_2O solution containing 1 wt % of a diffusing probe (in this case the star polymers) was added to poly(vinyl alcohol) (PVA) weighed in a 5-mm-o.d. NMR tube. The concentrations of the star polymers are much lower than their critical aggregation concentrations (CACs) determined by surface tension measurements.[21] The final concentrations of the matrix, PVA, ranged from 0 to 0.25 g mL^{-1}, at an increment of 0.05 g mL^{-1}. Molal concentration (mole of solute per 1000 g of solvent) is used in this work because of its convenience in the preparation of samples. Note that for dilute solutions, the

concentration in molality is close to that in molarity. The samples were sealed and heated at 110 $^{\circ}$C for 24 h.

2.3.3. NMR Measurements of Self-Diffusion Coefficients

The stimulated echo pulse sequence developed by Tanner (STE: 90-t_1-90-t_2-90-t_1-echo) was used to measure the self-diffusion coefficients (D) of the star polymers.[25] Measurements were performed at 23 $^{\circ}$C on a Bruker AV400 NMR spectrometer operating at a frequency of 400.27 MHz for protons. The self-diffusion coefficients (D) were obtained from the following relationship[26-28]

$$A = A_0 e^{-\gamma^2 \delta^2 G^2 D (\Delta - \delta/3)} \tag{2.1}$$

where A_0 and A are the NMR signals in the absence and in the presence of the gradient pulses of strength G, respectively, γ the gyromagnetic ratio of ^{1}H, δ the duration of the applied gradient pulses, and Δ the time interval between the two gradient pulses.

The interval Δ between the gradient pulses was fixed to 100 ms, the duration of the gradient pulse was set at 1 ms. The gradient strength was varied in 16 steps within a range from 0.1 to 10 T/m (the minimum and maximum varied depending on the system studied) to achieve an attenuation of at least 80% for the diffusants. The gradient was applied along the z axis. For selected samples, the self-diffusion coefficients were also measured in the x and y direction and the self-diffusion was found to be isotropic. The mean-squared displacement in one dimension can be estimated by $2D(\Delta - \delta/3)$. Since the typical self-diffusion coefficients are of the order of magnitude of 10^{-11} m^2/s, at Δ = 100 ms the root-mean-squared displacements are substantially larger than the radius of gyration of either monomeric diffusants or their micellar aggregates. Therefore, the self-diffusion coefficients measured by PGSE NMR experiments reflect the center-of-mass diffusion. The model of Petit *et al.*[29] was used to fit the experimental data. The coefficients of determination (R^2) obtained were in the range of 0.989−0.999.

2.3.4. T_1 Measurements

A standard inversion-recovery pulse sequence $(180^{\circ}_x - \tau - 90^{\circ}_x - \text{ACQ})$ was used to determine the longitudinal relaxation time (T_1) of the characteristic groups of the diffusants. The T_1 measurements at variable temperatures $(10 - 70\ ^{\circ}\text{C})$ were carried out on a Bruker AV400 NMR spectrometer. The T_1 measurements of the solutions with different concentrations were performed at 25 $^{\circ}\text{C}$. A total of 16 increments of the recovery delay times (τ) between 0.01 and 4 s were used and 8 scans were accumulated for all measurements.
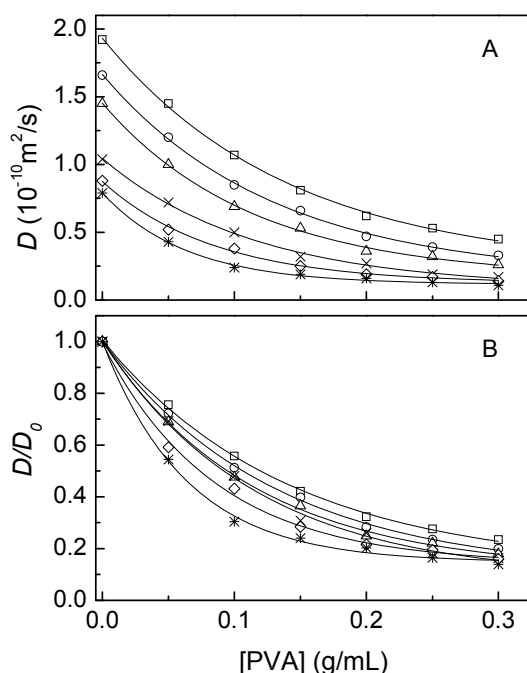
Figure 2.2. Self-diffusion coefficients (A) and reduced self-diffusion coefficients (B) of the star polymers as a function of PVA concentration at 25 $^{\circ}\text{C}$. CA(EG$_4$)$_4$, ($\square$); CA(EG$_6$)$_4$, ($\circ$); CA(EG$_{10}$)$_4$, ($\triangle$); CA(EG$_{17}$)$_4$, ($\times$); CA(EG$_{31}$)$_4$, ($\diamond$); CA(EG$_{39}$)$_4$, ($*$). The lines are fits to Eq. 2.2.

2.4. Results and Discussion

2.4.1. Diffusion Behaviors in PVA-Water-Diffusant Tenary Systems

Figure 2.2 shows the effect of PVA concentration on the self-diffusion coefficients of the star polymers. Both the increase in viscosity and hydrodynamic interactions contribute to the

substantial decrease in their diffusion coefficients with increasing PVA concentration. In the aqueous solutions, the hydrogen bonding between PVA and the ethylene glycol moieties can be neglected.[8] A higher PVA concentration generally means more obstructions for the diffusants.[30] The PVA network used in the study have a correlation length in the range of 0.4 – 3 nm,[5] which is smaller than or similar as the hydrodynamic radius, R_H, of the probes (1.3 – 3.1 nm, as obtained from Stokes-Einstein relation) (Table 2.2). Although the star polymers show similar trend as linear PEGs[6] and poly(propylene imine) dendrimers,[9] an increase in PVA concentration causes a larger decrease in the self-diffusion coefficient of the linear PEGs in comparison to the CA(PEG)$_4$ stars and the dendrimers of similar molecular weight.

The size of the diffusants has a clear effect on their self-diffusion coefficients in polymers.[6, 8-10, 13, 18] The self-diffusion coefficients D are normalized with their values in pure water (D_0) and the results in Figure 2.2B clearly show that the D/D_0 values decrease faster in the PVA concentration range of 0 – 0.15 g/mL with increasing MW of the star polymers. The change of diffusion coefficients is more significant for the molecules of higher molecular weight and larger size, which are expected to interact more extensively with the PVA matrix.

The experimental values of the self-diffusion coefficients as a function of PVA concentration can be fitted with the model of Petit $et\ al.$[29]

$$D = \frac{D_0}{1 + ac^{-\nu}} \qquad (2.2)$$

where $a = D_0/(k\beta^2)$, ν and β are constants which are characteristic of the polymer-solvent system, k represents the jump frequency over the energy barriers, which is expected to depend on the temperature and on the size of the diffusant, and c is the polymer concentration. In this model, the polymer solution is treated as a statistical network.

Table 2.2. Self-diffusion coefficients (D_0), hydrodynamic radii (R_H), and fitting parameters $k\beta^2$ and v obtained for the star polymers $CA(EG_n)_4$ in PVA-water-diffusant ternary systems

sample	M_n^a (g/mol)	D_0 (10^{-10} m²/s) exp.	D_0 (10^{-10} m²/s) calcd.[b]	$D_{s,0}$ (10^{-10} m²/s)	R_H (nm)[c]	v^b	$k\beta^2$ (10^{-11} m²/s)[b]
Star polymers							
$CA(EG_4)_4$	1110	1.92	1.92		1.28	0.65	1.17
$CA(EG_6)_4$	1510	1.66	1.66	1.60	1.48	0.66	0.82
$CA(EG_{10})_4$	2190	1.45	1.45		1.69	0.65	0.65
$CA(EG_{17})_4$	3500	1.04	1.04		2.36	0.70	0.35
$CA(EG_{31})_4$	5870	0.88	0.88	0.85	2.79	0.58	0.40
$CA(EG_{39})_4$	7320	0.79	0.79	0.78	3.10	0.56	0.31
Linear polymers							
PEG-600	1100 (530)	1.86	1.87		1.32	0.58	1.20
PEG-1000	1220 (970)	1.66	1.66		1.48	0.49	1.20
PEG-1500	1600 (1460)	1.13	1.13		2.17	0.54	0.68
PEG-2000	1960 (2140)	1.07	1.02		2.29	0.53	0.53
PEG-4000	4050 (4430)	0.96	0.96		2.55	0.50	0.47
PEG-8000	9100 (8000)	0.64	0.65		3.83	0.60	0.10
Dendrimers							
PPI(TEG)_8	2000	1.64	1.64		1.49	0.59	0.79
PPI(TEG)_{32}	8600	0.91	0.91		2.69	0.68	0.16
PPI(TEG)_{64}	17000	0.70	0.69		3.50	0.69	0.10

[a] For $CA(EG_n)_4$, the M_n values were measured by SEC-RI in THF. For linear PEGs, the M_n values were measured by SEC in THF and in water (values in parentheses).[6, 10] For the dendrimers, the M_n values were measured by ^{1}H NMR spectroscopy.[9] [b] Obtained as a fitting parameter from eq. 2.2. [c] Calculated from Stokes-Einstein equation.

The values obtained for the parameters, D_0, $k\beta^2$, and v are listed in Table 2.2. The D_0 values obtained from fitting agree well with the experimental data, with a clear dependence on the molecular size of the diffusants. The parameter v is dependent on the solvent and falls in the range of 0.50 – 0.70 for the ternary system, indicating water is a marginal solvent for PVA.[29] The parameter $k\beta^2$ decreases with increasing hydrodynamic radius of the diffusing star polymers (Table 2.2). Since β should remain constant for a given polymer-solvent system,[29] the results indicate that an increase in the size of the diffusant (R_H) leads to a lower jump frequency k. Similar decreasing trend was obtained with the linear PEGs[6] and PPI(TEG)$_n$ dendrimers.[9] At a comparable R_H value, the $k\beta^2$ parameter varies according to the general order of linear > star > dendrimer. This implies that the linear PEGs have a higher jump frequency than the diffusants in the other two series of comparable molecular size. When the R_H is larger than ca. 2 nm, the $k\beta^2$ values of both dendrimers and star polymers decrease more slowly since the movement of longer linear chains is hindered more substantially than the corresponding star-shaped polymers and dendrimers.
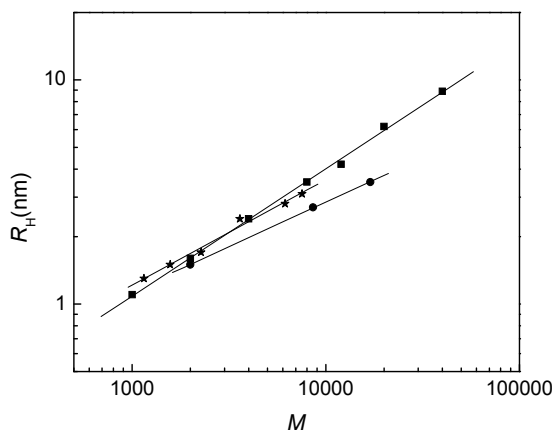
Figure 2.3. Logarithmic plot of the hydrodynamic radius R_H as a function of molecular weight for linear PEOs (■, data from reference[31]), dendrimers (●, data from reference[9]), and the star polymers (★) in aqueous solutions at 23 °C. Good linear relations were observed with the coefficients of determination (R^2) of 0.9983, 0.9998, and 0.9855, respectively.

2.4.2. Scaling Relation between the Hydrodynamic Radius and the Molecular Weight of the Diffusant in Water-Diffusant Binary Systems

Logarithmic plots of R_H versus M for linear PEOs, $CA(EG_n)_4$ star polymers, and the dendrimers are shown in Figure 2.3, with the slopes of the linear fitting being 0.57, 0.47, and 0.40, respectively. The star polymers essentially present a random coil conformation as some flexible linear polymers, whose scaling constant of the relation, $R_H \sim M^v$, falls in the range of 0.5 ~ 0.6.[15, 32, 33] Globular proteins,[34] star polymers,[35, 36] and dendrimers[37-40] normally have a scaling constant of 0.3 ~ 0.4 due to the globular shapes and the compact, space-filling nature. However, the scaling parameter of star polymers varies, and some star polymers such as 4 to 16-arm poly(ethylene oxide)s from carbosilane dendrimers have a scaling constant of 0.5.[41] Linear PEOs have slightly lower hydrodynamic radii than the corresponding $CA(EG_n)_4$ star polymers at low molecular weight due to the presence of a large cholane core in the star polymers. When the molecular weight is further increasing, R_H of the star polymers increases at a lower rate because the linear PEOs have a more extended structure in solution.[42] Since the molecular weights of star polymers are usually underestimated using SEC-RI calibrated with linear homologues,[43] SEC-LS was used to determine the absolute molecular weights of the star polymers. The comparison of the results obtained with both detectors shows that the absolute molecular weights measured by SEC-LS are 1.1 times of the values obtained by SEC-RI. Thus, the linear relation shown in Figure 2.3 also holds if the absolute molecular weights of the star polymers are used. The density of dendrimers is higher than those of branched and linear polymers due to their dense intramolecular packing, thus R_H increases slowly with higher M_n, as shown by $PPI(TEG)_n$ dendrimers in Figure 2.3. The observation agrees well with increasing molecular density of the dendrimers with higher generation numbers.[9]

Table 2.3. Molecular weights and hydrodynamic radii of the polymers shown in Figure 2.4A.

Polymer	M_n (g/mol)		R_H
	SEC	NMR	(nm)
CA(EG$_{31}$)$_4$	5870	8600	2.8
CA(EG$_{54}$)$_4$	9900	15460	4.1
Linear PEO-6k[a]	6000	6200	5.6
Linear PEO-10k[a]	10000	10600	7.1

[a] M_n and R_H values of the linear PEOs are from reference[20] and the same nomenclature is employed.

2.4.3. Effect of Diffusant Concentration on the Self-Diffusion Coefficient in Water-Diffusant Binary Systems

For a better understanding of the system, the self-diffusion coefficients of the probes were measured in the absence of a polymer matrix, with representative results of selected samples (Table 2.3) shown in Figure 2.4A. For the star polymers CA(EG$_n$)$_4$, the self-diffusion coefficient decreases significantly with increasing concentration of the diffusants in solution (Figure 2.4A). The decrease is more significant for those with higher molecular weights. de Gennes' prediction of a scaling regime $D \propto c^{-1.75}$ in semidilute solution[44] is not apparent in the molecular weight range from CA(EG$_6$)$_4$ (M_n = 1510 g/mol) to CA(EG$_{54}$)$_4$ (M_n = 9890 g/mol). No c^* (overlap concentration) can be defined for the star polymer of low molecular weights, such as CA(EG$_6$)$_4$. The self-diffusion coefficient of CA(EG$_6$)$_4$ decreases only slightly with increasing concentration. Similarly, previous work of Callaghan and Pinder showed that no semidilute regime was observed in the case of low MW linear polystyrene (MW = 2000) in CCl$_4$.[33]
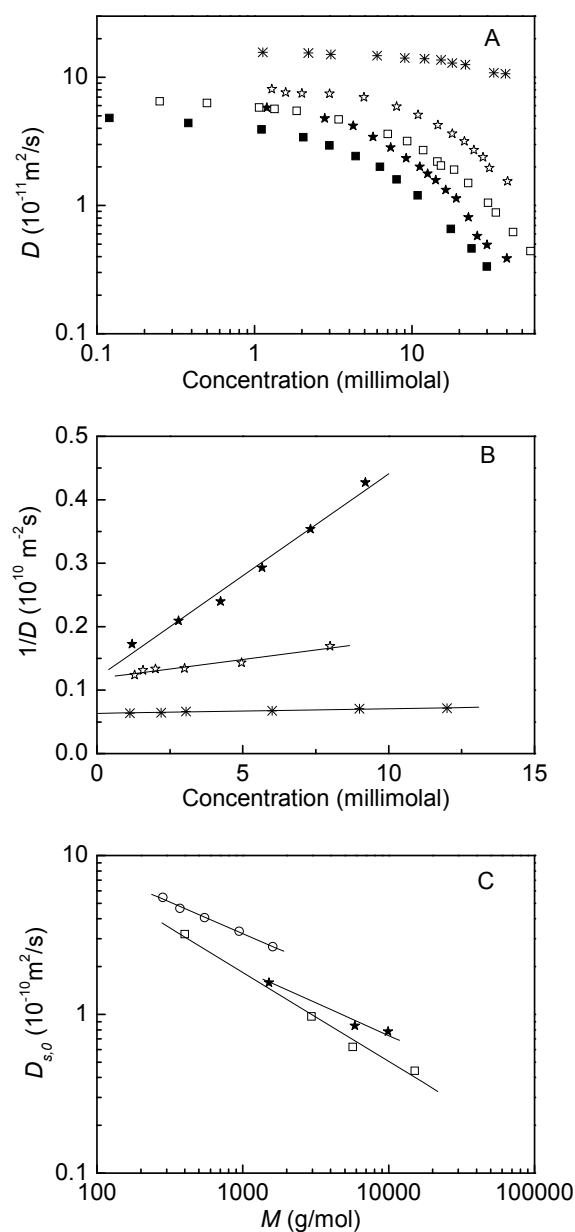
Figure 2.4. (A) The dependence of self-diffusion coefficient D on the concentration of polymer diffusants in water: CA(EG$_6$)$_4$ ($\ast$) (M_n = 1510), CA(EG$_{31}$)$_4$ ($\star$) (M_n = 5870), CA(EG$_{54}$)$_4$ ($\bigstar$) (M_n = 9890), linear PEO-6k ($\square$), linear PEO-10k ($\blacksquare$). Sample details are given in Table 2.3. Data of PEO-6k and PEO-10k are from reference.[20] (B) Variation of 1/D as a function of concentration of the star polymers. Sample details are given in Table 2.2. The lines are fits to Eq. 2.3 and the derived self-diffusion coefficient at infinite dilution ($D_{s,0}$) are shown in Table 2.2. (C) Variation of $D_{s,0}$ as a function of molecular weight of the star polymers in D$_2$O at 23 ^{o}C ($\bigstar$), linear PEGs in D$_2$O at 25 ^{o}C[45] ($\square$), and linear PEGs in D$_2$O at 30 ^{o}C[46] ($\circ$). A scaling behavior $D_{s,0} \sim M_n$ was observed with the scaling indices of 0.41, 0.60, and 0.43 for the star polymers and linear PEGs at 25 and at 30 ^{o}C, respectively.

34

For comparison purposes, Figure 2.4A also shows the literature data for linear PEOs.[20] The molecular weights and hydrodynamic radii of these polymers are summarized in Table 2.3. Diffusion coefficient measurements of two star polymers and two linear PEOs show similar decreasing trend within the concentration range of 0 – 40 millimolal. At very low concentrations (< 5 millimolal), $CA(EG_{54})_4$ (M_n = 9890) overlaps with linear PEO (M_n = 6000). At higher concentrations, the star-shaped diffusants showed slower diffusion than their linear homologues. Differences are expected between the star polymers and linear PEGs due to the presence of the hydrophobic core of the star polymers. Micelles can form in solutions above the CAC of the star polymers. According to surface tension measurements,[21] the CAC of $CA(EG_{31})_4$ is ca.19 millimolal and the value for $CA(EG_{54})_4$ may be slightly higher than this number because it is overall a more hydrophilic molecule. A comparison between $CA(EG_{17})_4$ and its *n*-alkyl poly(ethylene glycol) ether surfactant counterpart with similar molecular weight, $C_{17}EG_{84}$ (17 is the number of carbons in the alkyl chain and 84 the number of ethylene oxide units, with a CAC at 2.5 μM),[47] shows that $CA(EG_{17})_4$ (with a CAC at 16 millimolal) starts to aggregate at a much higher concentration. Therefore, at a similar molecular weight, the star polymer is much less hydrophobic than such a linear amphiphilic polymer and does not aggregate as easily.

A scaling relationship between the self-diffusion coefficient at infinite dilution and the molecular weight for a given diffusant, $D_{s,0} \propto M^{-n}$, originally proposed by Flory,[48] was observed for star polymers $CA(EG_n)_4$ dissolved in D_2O at 23 ^{o}C. The values of $D_{s,0}$ of $CA(EG_n)_4$ were determined from the initial linear region of a plot of D^{-1} versus c (Figure 2.4B) by fitting to the first-order expression of

$$D^{-1} = D_{s,0}^{-1}(1 + k_f c + ...) \tag{2.3}$$

where k_f and similar higher order coefficients are independent of c.[33] Logarithmic plots of $D_{s,0}$ versus molecular weight (Figure 2.4C) show that the $CA(EG_n)_4$ series has a scaling exponent *n* of 0.41. The scaling exponent of the star polymers is very close to the value of low molecular weight linear PEGs (monomer to N-mer of 40) at 30 ^{o}C (*n* = 0.43) reported in a study by Shimada *et al.*[46] The scaling factor obtained from another study by Blum *et al.* is 0.60 for linear PEGs in D_2O at 25 ^{o}C.[45] In this temperature range, the small differences in

temperature would have little effect on the self-diffusion coefficients of the polymers. The difference may be explained by the different molecular weight range (dimer to N-mer of 14,000) covered in the work of Blum et al.[45] and the high polydispersity for PEGs with high molecular weight. Similar to the cases of the linear and star PEGs, a report regarding linear and 3-armed polybutadienes showed no qualitative difference in self-diffusion coefficient between the two systems.[15]

2.4.4. The Longitudinal Relaxation Times of the Diffusants (T_1)

T_1 values provide additional information about the molecular dynamics of polymers in solution.[49] The ^{1}H NMR T_1 values of two polymers (CA(EG$_{31}$)$_4$ and CA(EG$_{54}$)$_4$) at different concentrations were measured at 23 $^{\circ}$C. With increasing concentration of the star polymers, the T_1 value of methylene protons on the PEG chain decreases while that of the methyl group protons on the cholane core increases slightly (Figure 2.5A). The changes of the T_1 values for the larger CA(EG$_{54}$)$_4$ are more pronounced. The temperature dependence of T_1 was also studied in order to clarify the relation between the mobility of the PEG moieties and the concentration of CA(EG$_n$)$_4$. In the range of 10 – 70 $^{\circ}$C, T_1 values of the methylene protons on the PEG segments of CA(EG$_{54}$)$_4$ at selected concentrations increase significantly with an increase in temperature, while those of the methyl protons of the cholane core first decrease and then increase within this temperature range (Figure 2.5B). In the Bloembergen-Purcell-Pound theory (BPP theory), T_1 shows a minimum along with the correlation time (τ_c, decreasing mobility).[50] The results indicate that these PEG methylene protons lie in the fast motion regime (where T_1 increases with increasing mobility), while the cholane core is in the intermediate motion regime (where T_1 is close to the minimum in the plot of T_1 vs τ_c). This mobility difference between the core and PEG chains of star polymers CA(EG$_n$)$_4$ is similar to that observed for the core and the exterior of poly(propylene imine) dendrimers,[51, 52] which suggests that the star polymers behave similarly in solution as the dendrimers. Star polymers CA(EG$_n$)$_4$ are amphiphilic and tend to form micelles in solution. However, no critical aggregation concentration or temperature was observed by NMR for such polymers. The micelles and the star polymers are in a dynamic process between free and aggregated states. The mobility reflected from the T_1 relaxation times is only an averaged observation.
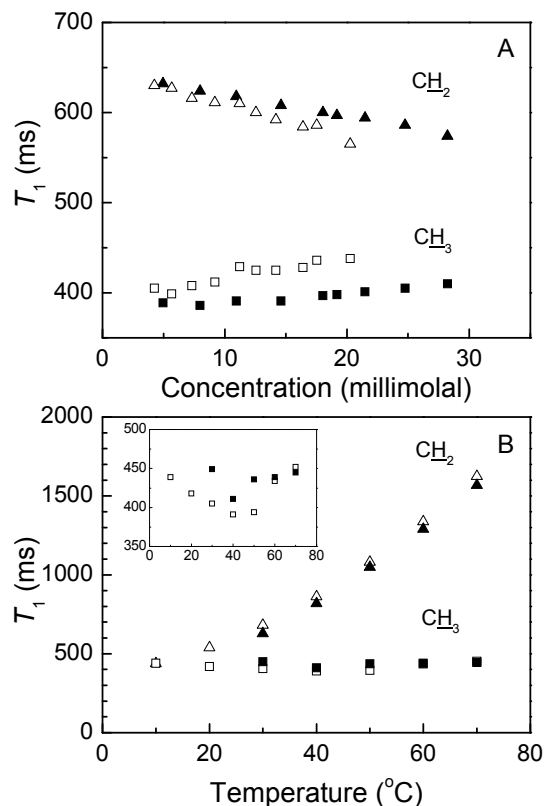
Figure 2.5. The ^{1}H T_1 values for CH_2 of PEG chains (triangles) and CH_3 of the cholane core (squares) measured for the star polymers. (A) Effect of concentration for two polymers $CA(EG_{31})_4$ (closed symbols), $CA(EG_{54})_4$ (open symbols) at 25 ^{o}C; (B) Effect of temperature for $CA(EG_{54})_4$ at 1.2 (open symbols) and 19.1 millimolal (closed symbols). The inset shows the variation of the T_1 values of CH_3 of the cholane core near the minimum with a different scale. The error of the T_1 values is estimated to be ± 10 ms by multiple experiments.

2.5. Conclusion

In an effort to understand the effect of molecular shape and architecture of polymeric diffusants on the diffusion in polymer hydrogels, we have compared the diffusion behaviors of PEG-based macromolecules including linear and star-shaped polymers and dendrimers in aqueous solutions and PVA gels. The results show that the star polymers have an intermediate diffusion rate or jump frequency that is higher than the dendrimers but lower than linear polymers at comparable hydrodynamic radii. In the dilute regime of the binary system, star polymers have the similar diffusion behavior as linear PEGs. In the semidilute

regime, a difference between the star polymers and their linear homologues is observed due to the presence of the hydrophobic core of the stars. For both 4-armed star polymers and linear PEGs, similar scaling relationships are found between the self-diffusion coefficient at infinite dilution and the molecular weight of the diffusants. The dependence of the ^{1}H T_1 values of the star polymers on temperature and concentration indicates that the cholic acid core of the star polymers is less mobile than the PEG arms. The understanding of the effect of molecular shape of the diffusants may help in designing molecules and biopolymers with predictable properties for applications such as drug delivery and tissue engineering.

2.6. Acknowledgements

2.7. References

1.   Hoare, T. R.; Kohane, D. S. *Polymer* **2008,** 49, 1993-2007.

2.   Fieber, W.; Herrmann, A.; Ouali, L.; Velazco, M. I.; Kreutzer, G.; Klok, H. A.; Ternat, C.; Plummer, C. J. G.; Manson, J. A. E.; Sommer, H. *Macromolecules* **2007,** 40, 5372-5378.

3.   Gao, P.; Fagerness, P. E. *Pharm. Res.* **1995,** 12, 955-964.

4.   Clericuzio, M.; Parker, W. O.; Soprani, M.; Andrei, M. *Solid State Ionics* **1995,** 82, 179-192.

5.   Petit, J.-M.; Zhu, X. X.; Macdonald, P. M. *Macromolecules* **1996,** 29, 70-76.

6.   Masaro, L.; Zhu, X. X.; Macdonald, P. M. *Macromolecules* **1998,** 31, 3880-3885.

7.   Masaro, L.; Ousalem, M.; Baille, W. E.; Lessard, D.; Zhu, X. X. *Macromolecules* **1999,** 32, 4375-4382.

8.   Masaro, L.; Zhu, X. X. *Langmuir* **1999,** 15, 8356-8360.

9.   Baille, W. E.; Malveau, C.; Zhu, X. X.; Kim, Y. H.; Ford, W. T. *Macromolecules* **2003,** 36, 839-847.

10. Thérien-Aubin, H.; Zhu, X. X.; Moorefield, C. N.; Kotta, K.; Newkome, G. R. *Macromolecules* **2007,** 40, 3644-3649.

11. Kharchenko, S. B.; Kannan, R. M.; Cernohous, J. J.; Venkataramani, S. *Macromolecules* **2003,** 36, 399-406.

12. Kharchenko, S. B.; Kannan, R. M. *Macromolecules* **2003,** 36, 407-415.

13. Baille, W. E.; Zhu, X. X.; Fomine, S. *Macromolecules* **2004,** 37, 8569-8576.

14. von Meerwall, E.; Tomich, D. H.; Hadjichristidis, N.; Fetters, L. J. *Macromolecules* **1982,** 15, 1157-1163.

15. von Meerwall, E.; Tomich, D. H.; Grigsby, J.; Pennisi, R. W.; Fetters, L. J.; Hadjichristidis, N. *Macromolecules* **1983,** 16, 1715-1722.

16. Furukawa, T.; Ishizu, K.; Yamane, Y.; Ando, I. *Polymer* **2005,** 46, 1893–1898.

17. Westrin, B. A.; Axelsson, A.; Zacchi, G. *J. Controlled Release* **1994,** 30, 189-199.

18. Michelman-Ribeiro, A.; Horkay, F.; Nossal, R.; Boukari, H. *Biomacromolecules* **2007,** 8, 1595-1600.

19. Gong, J. P.; Hirota, N.; Kakugo, A.; Narita, T.; Osada, Y. *J. Phys. Chem. B* **2000,** 104, 9904-9908.

20. Griffiths, P. C.; Stilbs, P.; Yu, G. E.; Booth, C. *J. Phys. Chem.* **1995,** 99, 16752-16756.

21. Luo, J.; Giguère, G.; Zhu, X. X. *Biomacromolecules* **2009,** 10, 900-906.

22. Gao, H.; Matyjaszewski, K. *Macromolecules* **2006,** 39, 7216-7223.

23. Breland, L. K.; Storey, R. F. *Polymer* **2008,** 49, 1154-1163.

24. Kennedy, J. P.; Jacob, S. *Acc. Chem. Res.* **1998,** 31, 835-841.

25. Tanner, J. E. *J. Chem. Phys.* **1970,** 52, 2523-2526.

26. Callaghan, P. T.; Trotter, C. M.; Jolley, K. W. *J. Magn. Reson.* **1980,** 37, 247-259.

27. Stilbs, P. *Prog. Nucl. Magn. Reson. Spectrosc.* **1987,** 19, 1-45.

28. Price, W. S. *Concepts Magn. Reson.* **1997,** 9, 299-336.

29. Petit, J.-M.; Roux, B.; Zhu, X. X.; Macdonald, P. M. *Macromolecules* **1996,** 29, 6031-6036.

30. Favre, E.; Leonard, M.; Laurent, A.; Dellacherie, E. *Colloids Surf., A* **2001,** 194, 197-206.

31. Choudhury, R. P.; Galvosas, P.; Schönhoff, M. *J. Phys. Chem. B* **2008,** 112, 13245–13251.

32. de Gennes, P. G. *J. Chem. Phys.* **1971,** 55, 572-579.

33. Callaghan, P. T.; Pinder, D. N. *Macromolecules* **1981,** 14, 1334-1340.

34. Tanford, C., *Physical Chemistry of Macromolecules*. John Wiley & Sons: New York, 1961.

35. Huang, H.-M.; Liu, I.-C.; Tsiang, R. C.-C. *Polymer* **2005,** 46, 955–963.

36. Trollsås, M.; Atthof, B.; Würsch, A.; Hedrick, J. L.; Pople, J. A.; Gast, A. P. *Macromolecules* **2000,** 33, 6423-6438.

37. Scherrenberg, R.; Coussens, B.; van Vliet, P.; Edouard, G.; Brackman, J.; de Brabander, E. *Macromolecules* **1998,** 31, 456-461.

38. Rietveld, I. B.; Bedeaux, D. *Macromolecules* **2000,** 33, 7912-7917.

39. Wong, S.; Appelhans, D.; Voit, B.; Scheler, U. *Macromolecules* **2001,** 34, 678-680.

40. Sagidullin, A. I.; Muzafarov, A. M.; Krykin, M. A.; Ozerin, A. N.; Skirda, V. D.; Ignat'eva, G. M. *Macromolecules* **2002,** 35, 9472-9479.

41. Comanita, B.; Noren, B.; Roovers, J. *Macromolecules* **1999,** 32, 1069-1072.

42. Devanand, K.; Selser, J. C. *Macromolecules* **1991,** 24, 5943-5947.

43. Taromi, F. A.; Grubisic-Gallota, Z.; Rempp, P. *Eur. Polym. J.* **1989,** 25, 1183-1187.

44. de Gennes, P. G. *Macromolecules* **1976,** 9, 587-593.

45. Waggoner, R. A.; Blum, F. D.; Lang, J. C. *Macromolecules* **1995,** 28, 2658-2664.

46. Shimada, K.; Kato, H.; Saito, T.; Matsuyama, S.; Kinugasa, S. *J. Chem. Phys.* **2005,** 122, 244914.

47. Hakansson, B.; Hansson, P.; Regev, O.; Soderman, O. *Langmuir* **1998,** 14, 5730-5739.

48. Flory, P. J., *Principle of Polymer Chemistry*. Cornell University Press: Ithaca, NY, 1953; p Chapter 14.

49. Mirau, P. A., *A Practical Guide of Understanding the NMR of Polymers*. John Wiley & Sons: Hoboken, New Jersey, 2005.

50. Hatada, K.; Kitayama, T., *NMR Spectroscopy of Polymers*. Springer-Verlag: Berlin Heidelberg, 2004.

51. Chai, M.; Niu, Y.; Youngs, W. J.; Rinaldi, P. L. *J. Am. Chem. Soc.* **2001,** 123, 4670-4678.

52. Malveau, C.; Baille, W. E.; Zhu, X. X.; Ford, W. T. *J. Polym. Sci., Part B: Polym. Phys.* **2003,** 41, 2969-2975.

3. NMR Imaging Study of Cross-linked High Amylose Starch Tablets: Effect of Drug Loading*

3.1. Abstract

NMR imaging techniques were used to study the effect of drug loading in cross-linked high amylose starch tablets. The tablets contained acetaminophen with loading levels from 10 to 40 wt%. The absolute amount of the drug released increased with larger amount of drug loading, but the percentages of drug released had only minor differences for the different tablets, probably due to the rapid formation of a gel layer for all the tablets, which slowed down drug release significantly. The releases of drugs from the tablets in all cases are dominated by a diffusion mechanism before the disappearance of the dry core of the tablets. Radial and axial swelling and water uptake were found to increase with the amount of drug loading. The diffusion rates of water were comparable at the initial stage for all the tablets with different loadings, but became faster later for the tables with higher amounts of drug loading as water diffusion may be facilitated by the hydrophilicity of the drug.

3.2. Introduction

Cross-linked high amylose starch (CHAS) has been demonstrated to be an effective controlled release matrix.[1-4] Once the CHAS tablets are hydrated, a consistent gel layer is formed very rapidly around the tablet core, leading to retarded release of drugs.[5] The integrity of the CHAS tablets is sustained for over 48 h.[6] We have used NMR imaging to study the effects of tablet size, temperature, and drug loading on the tablet swelling and water diffusion.[5-8] The effect of moisture content on the swelling of high amylose starch films was also studied using NMR imaging by Russo et al.[9] In addition, the conversion from V-type (single helix) to B-type (double helices) which limits the swelling of starch was also revealed by CP-MAS ^{13}C solid-state NMR spectroscopy.[10]

The drug release mechanism is classified into three cases: diffusion mechanism, polymer relaxation mechanism, and a mechanism which lies between the two cases. It was found for ethyl cellulose tablets that drug release is controlled by a diffusion mechanism at a high loading of acetaminophen (APAP) (49.5 wt %), while the effect of the polymer relaxation

becomes significant at a low loading (9.9 wt %).[11] In the case of poly(ethylene oxide) (PEO) tablets, the drug dissolution and diffusion through the swollen gel layer controlled the release at a loading levels of 39% and 20%, respectively.[12] Previously we have studied the release of two drugs, ciprofloxacin and acetaminophen, loaded at 10 wt% in CHAS.[5] The amount of drug loading may also have a significant effect on the amount released from the polymer tablets. APAP is an analgesic (pain reliever) and an antipyretic (fever reducer), which has been used as a probe to study controlled release properties of some matrices, including hydroxypropyl methyl cellulose (HPMC),[13] HPMC-polyvinylpyrrolidone,[14] and high-amylose sodium carboxymethyl starch matrices.[15] We also chose APAP in this study with loadings of 10, 20, and 40 wt % in the CHAS tablets. In vitro drug release from the matrix tablets was determined and the results were correlated with swelling and water uptake of the tablets. The diffusion coefficients of water can be obtained from profile fitting and diffusion-weighted NMR images.

3.3. Experimental

3.3.1. Preparation of Tablets

The polymer (CHAS) was made of chemically modified high amylose starch (70% amylose), cross-linked with 0.075 wt % phosphorous oxychloride in a mild alkaline medium first and further functionalized with 6 wt % of propylene oxide followed by washing and drying. Gelatinization of the starch under 160 ^{o}C and 5.5 bars was then conducted immediately prior to spray-drying. Appropriate amount of granulated acetaminophen (Compap, MW 151 g/mol, R_h 0.37 nm) and CHAS were mixed for 4 minutes. The blend was compressed to form tablets of 200 mg each with a dimension of 9.0 mm $\times$ 3.0 mm. To achieve the target weight and thickness for the tablets, the press parameters were adjusted to 1330 kg/cm^2 for 10 – 20 wt % drug loadings and 785 kg/cm^2 for 40 wt % drug loading along the axial direction. Dosages with drug loadings of 10, 20, and 40 wt % were obtained.

3.3.2. NMR Imaging

All NMR imaging experiments were carried out at 37.0 ^{o}C on a Bruker Avance-400 NMR spectrometer operating at a frequency of 400.27 MHz for protons equipped with a

microimaging probe having a 20 mm inner diameter. A standard spin–echo pulse sequence was used to obtain spin density images of the tablets in a 20 mm o.d. NMR tube containing 20 mL of distilled water. A slice of 0.5 mm in thickness was selected either perpendicular or parallel to the main magnetic field using a sinc-shaped pulse. Eight scans were accumulated to obtain 128×128 pixel images for a field of view of 2.0 cm, leading to an in-plane resolution of 156 μm. An echo time (TE) of 3 ms and a repetition time (TR) of 1 s were fixed leading to an acquisition time of about 17 min for each image.

Diffusion-weighted images were acquired by combining the spin-echo pulse sequence with the pulsed-gradient spin-echo (PGSE) pulse sequence developed by Stejskal.[16] The diffusion time (Δ) and the length of the gradient pulse (δ) were 10 ms and 2 ms, respectively. The gradient strength varied from 5 to 100 G/cm.

3.3.3. Solubility Tests of CHAS

The CHAS powder (300 mg) was mixed with 20 mL distilled water in a 50 mL centrifuge tube, which was then placed in a shaking bath and agitated at 100 rpm and 37 ^{o}C for 30 minutes. The samples were centrifuged (4000 rpm, 1 h) and the supernatant was collected and dried at 70 ^{o}C for soluble fraction quantification. The test was performed in triplicate.

3.3.4.Water Uptake Experiments

Water uptake studies were carried out in a water bath at 37 ^{o}C with mild agitation. Each tablet was immersed in 20 mL distilled water and the weight was measured in triplicate at predetermined time intervals. The percentage of mass uptake is defined as

$$S_t = \frac{M_t - M_0}{M_0} \times 100\% \qquad (3.1)$$

where S_t is the water uptake in percentage, M_0 and M_t are the initial weight of a tablet and its weight at time t, respectively.

3.3.5.In Vitro Drug Release Tests

The tablets were placed individually in 900 mL of distilled water at 37 ^{o}C in a U.S.P.

XXIV dissolution apparatus 2 (Distek Premiere 5100 dissolution system) equipped with a rotating paddle (100 rpm). The amount of drug released from the tablet in a 24-h period was determined spectrophotometrically (244 nm) at an interval of 30 min. The sampling liquid flowed back to the vessels. All tablets were tested in triplicate.

The fitting of the data from NMR imaging experiments and of the drug release tests was carried out with Microsoft Excel 2003 using the Newton method to minimize the sum of the squared errors. A summation of 30 roots of the Bessel function was used.

3.4. Results and Discussion

Figure 3.1 shows the NMR images of CHAS tablets acquired from 1 to 20 h in water at 37 $^{\circ}$C. A gel layer formed quickly within a few minutes after the tablets came into contact with water. All three images at 1 h clearly show the gel layer, the hydrated layer, and the dry core (with the lowest water signal). The formation of the gel layer is essential for the controlled release of the CHAS tablets. The apparent high water signal shown by the periphery of tablets is caused by the shorter longitudinal relaxation time T_1 (ca. 800 ms) of the hydrated layer compared with that of the free water (ca. 5 s). As the water front advanced towards the center, the dry core gradually diminished in dimension with immersion time. The effect of drug loading levels is visible on the images acquired at 5 h and onward. At 20 h, water is distributed almost evenly in the tablet of 40% APAP, while the tablet of 10% APAP is still far from reaching equilibrium (Figure 3.1). NMR imaging experiments showed the tablets with 10% APAP loading reached equilibrium after 50 h. Therefore, the diffusion of water inside the tablets depends on the amount of APAP inside. It is to be noted that the movement of water into the tablet in the presence of the drug may not be strictly diffusional as the contribution of osmotic convection at the beginning stages of the process is present.

Figure 3.2A shows the mass uptake of tablets. Overall, the amount of mass change is contributed by the weight gain due to water diffused into the tablets and the weight loss due to drug release from the tablets. The solubility of CHAS in water (2.6 mg/mL) is much lower than that of APAP (14.5 mg/mL, USP XXIV) so that the amount of dissolved CHAS can be neglected, but frequent manipulations may also cause weight loss and thus the mass uptake may be underestimated. In general, the tablets with higher amount of drug loading had a lower gain in mass. The difference between the mass uptake at equilibrium is close to the

difference between drug loading level. The tablet with low drug loading had a faster increase in mass and reached an equilibrium earlier in time. Clearly, the tablets of 40% APAP undergo the highest weight loss due to drug release. In addition, the gel layers formed on these tablets are softer than the gel layers formed on tablets with lower drug loading levels, which is clearly visible, so that these layers are less resistant to erosion.
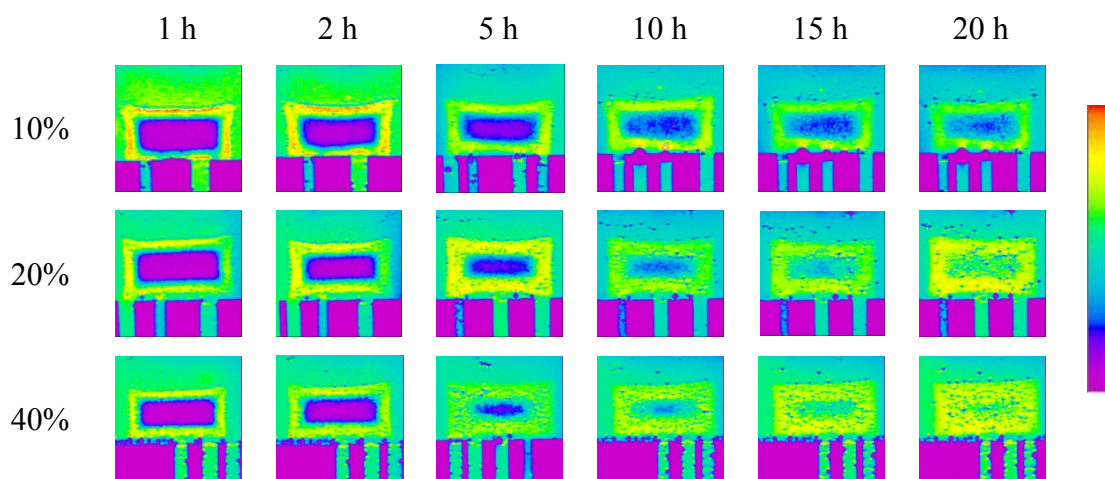
Figure 3.1. NMR images of CHAS tablets immersed in water at 37 $^{\circ}$C for 1, 2, 5, 10, 15, and 20 h. The part at the bottom of images is the Teflon support.

Table 3.1. The initial diffusion coefficients of water fitted to Eq. 3.2 and the average diffusion coefficients fitted to Eq. 3.5 in the CHAS tablets.

drug loading (%)	axial D_0 (10^{-11} m$^2 \cdot$ s^{-1})	radial D_0 (10^{-11} m$^2 \cdot$ s^{-1})	$\bar{D}_0$ (10^{-11} m$^2 \cdot$ s^{-1})	$\bar{D}_\infty$ (10^{-11} m$^2 \cdot$ s^{-1})
10	6.5 ± 0.2	5.2 ± 1.1	2.4 ± 0.2	13.6 ± 2.1
20	7.1 ± 0.4	3.3 ± 0.6	1.82 ± 0.04	12.3 ± 0.1
40	7.6 ± 0.3	4.2 ± 0.5	2.0 ± 0.2	16.2 ± 2.5

Figures 3.2B and 3.2C show the radial and axial swelling of the tablets, respectively. The axial swelling is almost 3 times of the radial swelling for all the tablets, which has been observed for the CHAS tablets with and without the drug.[5, 6] The higher axial swelling is caused by the compression along the axial direction during the preparation process. To

prevent the floating and movements of the tablets in the liquid media, a piece of cotton ball was placed above the tablet to keep it in place during the NMR imaging experiments, which may have caused the relatively higher standard deviations of axial swellings in comparison to those of radial swellings. The tablets with 10% loading has the lowest swelling, while the other two swell at a similar rate and reached a similar size. The drug APAP has a higher hydrophilicity than the matrix, which facilitates the penetration of water and enhances the overall swelling in both axial and radial directions.

The measurement of diffusion coefficients of water (D) inside of the CHAS tablets may provide quantitative information on the effect of drug loading on the mobility of the polymer matrix. The initial diffusion coefficient of water can be obtained from the water proton image profiles, an example of which is shown in Figure 3. At the initial stage of swelling, a tablet can be treated as an infinite cylinder in which water diffusion follows Fick's second law of diffusion.[6, 17] The initial diffusion coefficients of water (shown in Table 3.1) can be obtained from fitting the data to

$$\frac{C}{C_0} = 1 - 2\sum_{n=1}^{\infty} \frac{J_0(x\alpha_n / r)}{\alpha_n J_1(\alpha_n)} e^{\left(-D\frac{\alpha_n^2}{r^2}t\right)} \tag{3.2}$$

where C and C_0 are the concentrations of water at distance x and at the surface of the cylinder, respectively, r is the radius of the cylinder, D the diffusion coefficient of water, t the immersion time, J_0 Bessel function of the first kind of the order 0, J_1 the Bessel function of the first kind of the order 1, and α_n the nth root of $J_0 = 0$.[18-21]

At the beginning of immersion, the assumption of infinite cylinder is applicable and good fits to Eq. 3.2 can be easily obtained, as exemplified by Figure 3.3. The initial diffusion coefficients of water in CHAS tablets are comparable for all three tablets with different drug loading levels along both directions (Table 3.1). But significant deviations from the model were observed with the further advancement of water inside the tablets. Alternatively, the average diffusion coefficient ($\bar{D}$) can be calculated from mass uptake by substituting the k_d value obtained from Eq. 3.3 into Eq. 3.4:[17, 22]

$$\frac{M}{M_\infty} = k_d t^n \tag{3.3}$$

$$\bar{D} = \left(\frac{k_d \pi r}{4} \right)^2 \tag{3.4}$$

where M and M_∞ are the amounts of water penetrated in a tablet at time t and at equilibrium, respectively, and k_d is a parameter related to the diffusion.
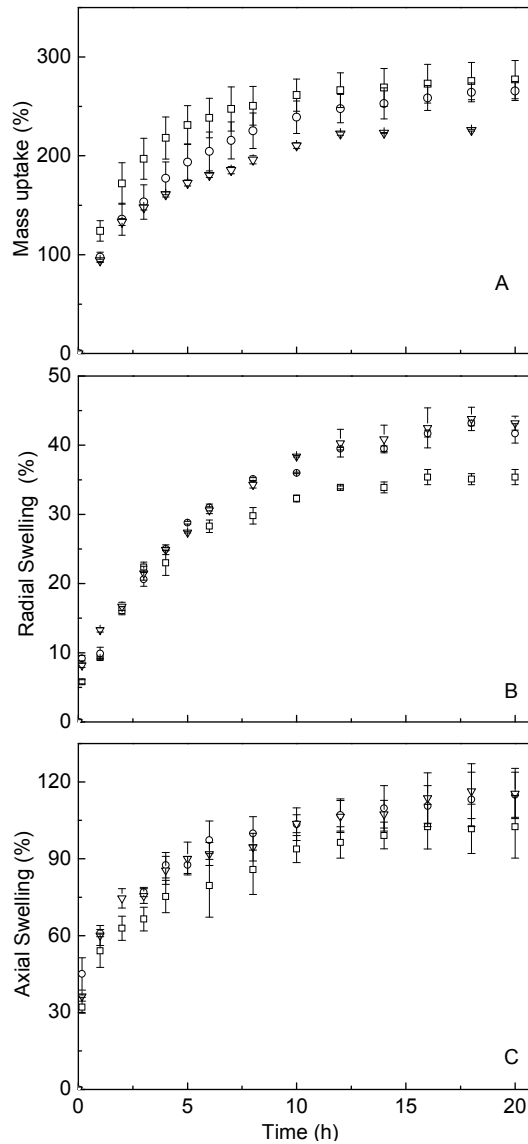

Figure 3.2. Mass uptake (A), radial swelling (B), and axial swelling (C) of the CHAS tablets loaded with 10% (□), 20% (○), and 40% acetaminophen (∇). Note that the mass uptake is the combined effect of mass gain by the absorption of water and the mass loss by the release of the drug.
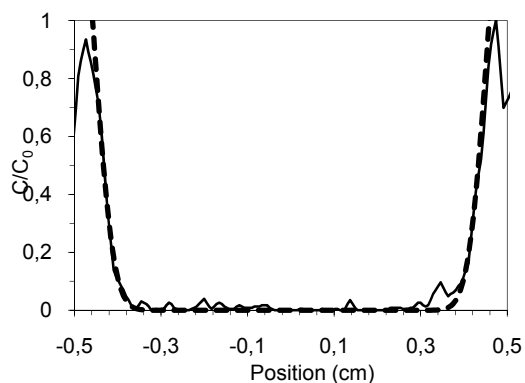
Figure 3.3. The water proton spin density profile (solid line) and the fit to Eq. 3.2 (dashed line) of a CHAS tablet with 20% acetaminophen swelled in water at 37 $^{\circ}$C for 30 min.

Mass uptake could be obtained from either gravimetric analyses or the integration of water signals in NMR images. The tablets become fragile after immersion in water, and manipulations during the weighing process may introduce errors, yielding less consistent results than the integration of signals of the NMR images. The latter method may be also difficult to apply for the system here, since Eq. 3.3 becomes invalid at ca. 60% of water uptake,[9, 23] which can be accomplished within 3 h for the tablets. The rapid water uptake during the first 3 h and the long acquisition time of each image with good S/N ratio (17 min) add up to the difficulty of obtaining an accurate $\bar{D}$.

To overcome such difficulties, diffusion-weighted images were acquired from which average diffusion coefficients may be obtained. This method produces images weighted with the local characteristics of water diffusion. The diffusion coefficients of both the gel part and the core of the tablets with various drug loading levels are shown in Figure 3.4. Reliable values of D cannot be obtained for an immersion time of less than 10 h when the signal attenuation is too low to be accurately detected even if a high gradient strength is applied. The figure shows that the self-diffusion coefficients of water in the outer gel changes only slightly with time and the values are comparable for different tablets, while those in the inner part of the tablets changed with time and vary significantly with different drug loading levels. The signal in the core for the tablets with 40% drug loading increased faster than the tablets of lower loadings. The faster water diffusion in these tablets agrees well with the faster swelling of the tablets. Since APAP is more hydrophilic than the CHAS matrix, a higher loading of

48

APAP facilitates the diffusion of water towards the core.
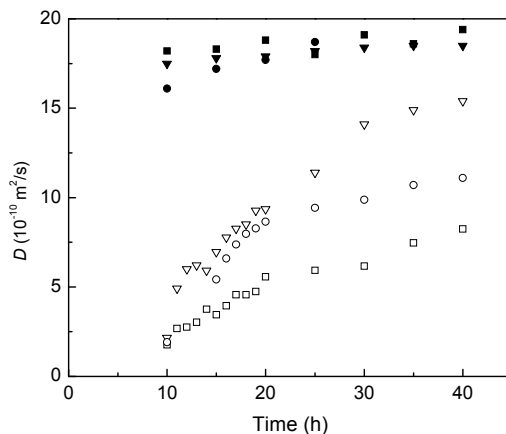
Figure 3.4. Diffusion coefficients of water in the inner core of the tablets loaded with 10% (□), 20% (○), and 40% acetaminophen (∇) obtained by diffusion-weighted imaging. The values corresponding to the hydrated gels of the tablets are shown by closed symbols.

The percentage of drug released at 37 $^{\circ}$C (Figure 3.5A) shows only minor difference among the tablets of different drug loading levels, even though the absolute amount of the drug released are very different (Figure 3.5B). A small initial burst could be attributed to release of the drug at the surface and surface erosion of the matrix prior to the formation of a gel layer. The drug release curves can be fitted to the equation $F = k\,t^{n}$. The value of power index n serves as a criterion to determine whether the release is controlled by a diffusion mechanism ($n = 0.5$) or polymer relaxation mechanism ($n = 1$). For the CHAS tablets with 10, 20, and 40% APAP, the n values are found to be 0.51, 0.55, and 0.56, respectively, indicating the drug release process is dominated by a diffusion mechanism in all the tablets.
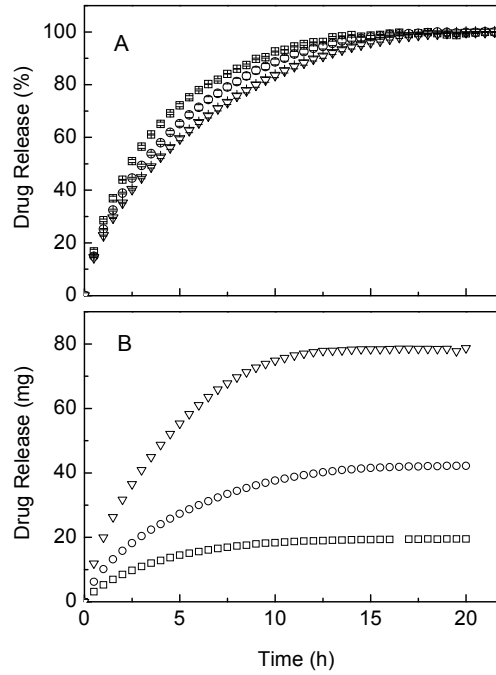
Figure 3.5. Release of drugs of CHAS tablets loaded with 10% (□), 20% (○), and 40% acetaminophen (∇). The amount of the drug released is quite different while the percentage remained similar.

The average diffusion coefficients ($\bar{D}$) may be obtained by fitting the dissolution test results to the following equation:[24]

$$\frac{M(t)}{M(\infty)} = 1 - \frac{8}{l^2 a^2} \sum_m \alpha_m^{-2} \exp(-D\alpha_m^2 t) \sum_n \beta_n^{-2} \exp(-D\beta_n^2 t) \qquad (3.5)$$

where *M(t)* and *M(∞)* are the amounts of drug released at time *t* and infinite time, respectively; *l* is the half-thickness of the tablet, *r* the radius, *D* the diffusion coefficient; α and β are parameters defined in $J_0(r\alpha) = 0$ and $\beta_n = \frac{(2n+1)\pi}{2l}$, where J_0 is a zero-order Bessel function. The model is applicable to tablets of a shape ranging from a flat disk to a cylinder. It is important to note that the validity of the equation is based on the hypotheses that there is no dimension change of the tablets, no variation of the diffusion coefficient of water from outer gel to inner core, and no gradual increase of diffusion coefficients of water

in the tablets over time. For comparison purposes, the fitting was performed on two stages, yielding the "initial" average diffusion coefficient ($\bar{D}_0$) using initial dimension of the tablet (l and r) during the drug release of $0 - 60\%$ (corresponding to an immersion time from 0 to 3.5 and 4 hours depending on the amount of drug loading) and the average diffusion coefficient at equilibrium ($\bar{D}_\infty$) using the final dimension during the drug release of $80 - 100\%$, corresponding to an immersion time period of ca. 7 to 18 hours. The results are shown in Table 3.1. The assumption of a constant diffusion coefficient leads to lower $\bar{D}_0$ values than those obtained by spin density profile fitting, but still in the same order of magnitude. Moreover, the values for $10 - 40\%$ drug loadings are similar to each other, which is consistent with the trend obtained from NMRI profile fitting. At equilibrium, the water diffuses much faster than at the beginning and thus $\bar{D}_\infty$ is almost an order of magnitude higher than $\bar{D}_0$. The trend is also reflected by the diffusion-weighted imaging experiments (Figure 3.4). The difference between the two series of diffusion coefficients may be explained by the low repetition time used during the diffusion-weighted imaging experiments.

3.5. Conclusion

We study the effect of drug loading for the case of cross-linked high amylose starch with APAP. In this case, the amount of the drug released is higher with a higher level of drug loading, but the percentage of the drug remained similar, making the prediction of drug release easier. This is likely due to the formation of a protective gel layer upon hydration of the tablets, which serves as a key factor in such a controlled release process. The NMR imaging results also show that the radial and axial swelling and water uptake of the CHAS tablets increased with the drug loading level. Diffusion of water is faster for the tables of high drug loadings due to the hydrophilicity of APAP, especially at a later stage of the release process. The dissolution tests demonstrated that the release of APAP from the CHAS tablets followed a diffusion mechanism.

3.6. Acknowledgements

3.7. References

1. Mateescu, M. A.; Lenaerts, V.; Dumoulin, Y. Use of cross-linked amylose as a matrix for the slow release of biologically active compounds U. S. Patent 5,456,921, Oct.10, 1995.

2. Dumoulin, Y.; Alex, S.; Szabo, P.; Cartilier, L.; Mateescu, M. A. *Carbohydr. Polym.* **1998,** 37, 361-370.

3. Lenaerts, V.; Moussa, I.; Dumoulin, Y.; Mebsout, F.; Chouinard, F.; Szabo, P.; Mateescu, M. A.; Cartilier, L.; Marchessault, R. *J. Control. Release* **1998,** 53, 225-234.

4. Lenaerts, V.; Beck, R. H. F.; Van Bogaert, E.; Chouinard, F.; Hopcke, R.; Desevaux, C. Cross-linked high amylose starch for use in controlled-release pharmaceutical formulations and processes for its manufacture. U.S. Patent 6,607,748, August 19, 2003.

5. Thérien-Aubin, H.; Zhu, X. X.; Ravenelle, F.; Marchessault, R. H. *Biomacromolecules* **2008,** 9, 1248-1254.

6. Thérien-Aubin, H.; Baille, W. E.; Zhu, X. X.; Marchessault, R. H. *Biomacromolecules* **2005,** 6, 3367-3372.

7. Baille, W. E.; Malveau, C.; Zhu, X. X.; Marchessault, R. H. *Biomacromolecules* **2002,** 3, 214-218.

8. Malveau, C.; Baille, W. E.; Zhu, X. X.; Marchessault, R. H. *Biomacromolecules* **2002,** 3, 1249-1254.

9. Russo, M. A. L.; Strounina, E.; Waret, M.; Nicholson, T.; Truss, R.; Halley, P. J. *Biomacromolecules* **2007,** 8, 296-301.

10. Thérien-Aubin, H.; Janvier, F.; Baille, W. E.; Zhu, X. X.; Marchessault, R. H. *Carbohydr. Res.* **2007,** 342, 1525-1529.

11. Neau, S. H.; Howard, M. A.; Claudius, J. S.; Howard, D. R. *Int. J. Pharm.* **1999,** 179, 97-105.

12. Kim, C.-J. *Drug Dev. Ind. Pharm.* **1998,** 24, 645-651.

13. Cao, Q. R.; Choi, Y. W.; Cui, J. H.; Lee, B. J. *J. Control. Release* **2005,** 108, 351-361.

14. Ebube, N. K.; Hikal, A. H.; Wyandt, C. M.; Beer, D. C.; Miller, L. G.; Jones, A. B. *Pharm. Dev. Technol.* **1997,** 2, 161-170.

15. Nabais, T.; Brouillet, F.; Kyriacos, S.; Mroueh, M.; da Silva, P. A.; Bataille, B.; Chebli, C.; Cartilier, L. *Eur. J. Pharm. Biopharm.* **2007,** 65, 371-378.

16. Stejskal, E. O.; Tanner, J. E. *J. Chem. Phys* **1965,** 42, 288-292.

17. Crank, J., *The Mathematics of Diffusion.* 2nd ed.; Oxford University Press: Oxford, 1975.

18. Ghi, P. Y.; Hill, D. J. T.; Maillet, D.; Whittaker, A. K. *Polymer* **1997,** 38, 3985-3989.

19. Chowdhury, M. A.; Hill, D. J. T.; Whittaker, A. K. *Biomacromolecules* **2004,** 5, 971-976.

20. Chowdhury, M. A.; Hill, D. J. T.; Whittaker, A. K.; Braden, M.; Patel, M. P. *Biomacromolecules* **2004,** 5, 1405-1411.

21. George, K. A.; Wentrup-Byrne, E.; Hill, D. J. T.; Whittaker, A. K. *Biomacromolecules* **2004,** 5, 1194-1199.

22. Alfrey, T. J.; Gurnee, E. F.; Lloyd, W. G. *J. Polym. Sci. Polym. Symp.* **1966,** 12, 249-261.

23. Ghi, P. Y.; Hill, D. J. T.; Whittaker, A. K. *Biomacromolecules* **2001,** 2, 504-510.

24. Fu, J. C.; Hagemeir, C.; Moyer, D. L. *J. Biomed. Mater. Res.* **1976,** 10, 743-758.

4. Swelling Behavior of Chitosan, Carboxymethyl Starch and Chitosan-Carboxymethyl Starch Mixture As Studied by NMR Imaging*

4.1. Abstract

The swelling properties of the tablets made of chitosan, carboxymethyl starch and a polymer complex based on a mixture of these two polysaccharides were studied by NMR imaging. Water and simulated physiological fluids were used to study the effect of pH and ionic strength on the swelling of the tablets and on the diffusion of fluid into the tablets. The tablets were compared also with those made of cross-linked high amylose starch. The capacities to modulate the release rate of drugs in different media was discussed by comparing the matrices and evaluating the preparation process of the complex.

4.2. Introduction

Polysaccharides are among the most abundant macromolecules in nature and present several advantageous characteristics for various applications. They are highly stable, non-toxic, hydrophilic, biodegradable and some of them bioadhesive. The presence of hydroxyl groups or amine groups in polysaccharides allows for chemical derivatization and cross-linking. Improved physicochemical properties can be achieved by chemical modifications. For these reasons, drug delivery with solid oral dosage forms has often used polysaccharides, such as starch, cellulose, chitosan, collagen and pectin. For example, hydroxypropyl methylcellulose (HPMC) is one of the most widely used polymer carriers in the pharmaceutical industry. The ratio of hydroxypropyl groups to methoxyl groups can be modified to produce HPMC products of different hydrophilicities.[1]

Cross-linked high amylose starch (CHAS) is an excellent excipient for controlled drug release because the cross-linking keeps the polymeric network from erosion and retrogradation and more importantly, restrains swelling of the matrix. The sustained release was optimized for a CHAS matrix with a cross-linking degree of 6% (often defined as the

weight ratio of the cross-linking agent to the starch).[2] The pK_a of natural starch is about 12-14.[3, 4] Therefore, pH has no effect on the swelling of the CHAS tablets at pH 2-8 in the gastrointestinal tract. Carboxymethyl starch (CMS), on the other hand, is an anionic polymer with a pK_a of about 4.8[5] due to the presence of carboxyl groups.[6, 7] So that its swelling is suppressed in gastric fluid. The resultant oral dosage forms could decrease irritation to stomach caused by soluble drugs and increase their bioavailability. In intestine surroundings, CMS is deprotonated and the polymer chains swell, leading to the release of the drug entrapped in the matrix. CMS was proposed as a pharmaceutical excipient for oral dosage forms of bioactive agents such as peptides,[8] enzymes[9] and probiotics.[10] In contrast to starch, chitosan is a linear cationic polysaccharide due to the presence of amine groups. Its pK_a value is about 6.3.[11] In acidic media, unmodified chitosan dissolves due to protonation of its amine groups. The control of drug release depends on the dissolution rate and this can be modulated by the formulation of excipients.

The pH-dependent drug release can cause *in vivo* variability, and thus it is difficult to correlate *in vitro* release with *in vivo* drug availability. Complexation represents an effective way to modulate the pH-sensitive swelling of polyelectrolytes. A complex can be formed in the presence of chitosan and a polyanionic polymer (such as polysaccharides,[12] synthetic polymers,[13] proteins[14] and DNA[15]).[16] The complexation occurs without cross-linking agents, catalysts or organic solvents, which alleviates the concerns about safety in the body.[16, 17] In this study, the complex of CMS and chitosan obtained by direct precipitation has been investigated.

In general, the water uptake properties of anionic and cationic polymeric excipients are provided by the ionization of the functional groups, which depends on the pH and on the ionic strength of the external medium.[18] Although the effect of pH on the swelling of the above-mentioned four excipients, CHAS, CMS, chitosan and CMS-chitosan complex, is qualitatively predictable, a quantitative study will generate useful information on their capabilities to control the drug release. The hydration data will also serve to the modulation of the excipient preparation for better reproducibility.

Nuclear magnetic resonance imaging (NMRI) is one of the ideal methods to record *in situ* the swelling behavior of solid oral dosage forms, thanks to its noninvasive and nondestructive nature. Magnetic field gradients are used to encode the spatial distribution of

the spin density.[19] Researchers can use NMRI to evaluate the polymer concentration profile during the swelling of the tablets,[20, 21] quantify dimensional properties (thickness, area and volume) during the swelling,[22-26] and define the diffusion front by a sharp gradient in signal intensity.[22, 23] Furthermore, the NMRI studies can provide the diffusion coefficient of a liquid component,[25, 26] and the spin-lattice and spin-spin relaxation times which relate to the environment of the penetrant and its physical bonding to the polymer system.[27]

We have used NMRI in the study of the CHAS tablets with and without loaded drugs,[22-26, 28] and investigated the effect of temperature, tablet size and the drug loading on the swelling and water uptake of the CHAS tablets. In this study, we would like to compare the characteristics of the tablets of the four matrices in three different media, i.e., simulated gastric fluid (SGF), simulated intestinal fluid (SIF) and water. This should provide a better understanding of the polysaccharides used in drug delivery systems. CHAS, a well-characterized polymer matrix for sustained release of drugs, served as a basis of comparison in the study of the other three matrices.

4.3. Experimental Section

4.3.1. Preparation of Matrices and Tablets.

High amylose starch (corn starch Hylon VII) was obtained from National Starch Co. and cross-linked at 6% with epichlorohydrin as reported.[2] The CMS was prepared by the alkali-catalyzed reaction of the high amylose corn starch with chloroacetic acid as previously described.[29, 30] The degree of substitution of CMS determined by back-titration method is about 0.14.[30] Chitosan (Marinard Biotech, Rivière-au-Renard, QC, Canada) was purified by solubilization in acetic acid followed by filtration.[30] The degree of deacetylation of the chitosan was about 80% according to acid-base titration and its approximate molecular weight determined by Mark-Houwink-Sakurada method was about 700 kDa.[30] A stoichiometric CMS-chitosan complex was prepared by coagulation of CMS and chitosan in an aqueous medium. The interpolymer complex contains 14 wt% of chitosan. The unloaded tablets of 200 mg were obtained by direct compression (2.5 tonnes) of the excipient powder. Flat-faced punches and a Carver hydraulic press were used to obtain tablets of 9.6×2.1 mm.

4.3.2. Preparation of Media.

Simulated gastric fluid (SGF) and simulated intestinal fluid (SIF) were prepared according to USP XXIV,[31] without pepsin nor pancreatin being added. SGF (pH 1.2) was prepared by dissolving 2.0 g of NaCl in 7 mL of HCl, followed by dilution to 1000 mL. SIF (pH 6.8) was prepared by dissolving 6.8 g of KH_2PO_4 in 250 mL of distilled H_2O, and adding 77 mL of 0.2 M NaOH solution followed by dilution to 1000 mL with distilled water.

4.3.3. NMR Imaging.

All NMR imaging experiments were carried out at 37.0 ^{o}C on a Bruker Avance-400 NMR spectrometer operating at a frequency of 400.27 MHz for protons equipped with a microimaging probe with a 20 mm inner diameter. A standard spin-echo pulse sequence was used to obtain spin density images of each tablet in the 20 mm o.d. NMR tube containing 20 mL of the media (distilled water, SGF, or SIF). A slice of 0.5 mm in thickness was selected either perpendicular or parallel to the main magnetic field using a sinc-shaped pulse. Eight scans were accumulated to obtain 128 × 128 pixel images for a field of view of 2.0 cm, leading to an in-plane resolution of 156 μm. An echo time (TE) of 3 ms and a repetition time (TR) of 1 s were fixed, leading to an acquisition time of about 17 min for each image.

In addition to observing the tablets swell in the same medium until equilibrium, some tablets were studied by changing the media: first observing the tablets in SGF for 2 h and then in SIF until swelling equilibrium was reached. This was used to simulate the situation of a tablet's transit through the gastrointestinal tract, which is denoted as SGF-SIF hereafter.

4.4. Results and Discussion
4.4.1 NMR Imaging and Proton Density Profiles.

NMR imaging provides a visual representation of the spatial distribution of water by acquiring signals directly from the protons. Figure 4.1 presents the NMR images of tablets based on the CMS-chitosan complex in media of different pH values. The images of the tablets made of other excipients are shown in Figures 4.4 - 4.6 in the Supporting Information. The image cross-sections clearly demonstrate the time-dependent ingress of water into the

polymer matrix. Moreover, the swelling of a tablet in the fluid can be visualized from the NMR images. ^{1}H tuning and matching strongly depend on the ionic strength of the sample. A buffer solution, such as SGF, often causes de-tuning of the probe and some artifacts in the NMR images of the highly ionic samples,[32, 33] as observed in some images in Figure 4.1. The higher intensity of the water inside the tablets is attributed to the different longitudinal relaxation time (T_1), 5 s for the bulk water vs. 800 ms for the water inside the tablet. The repetition time was fixed at 1 s, so that all the images obtained are T_1-weighted. The magnetization of the bulk water does not have enough time to return to equilibrium, contrary to the magnetization of water inside the tablet, leading to a higher proton signal intensity than that of the bulk water initially at the interface of the tablet and aqueous media.
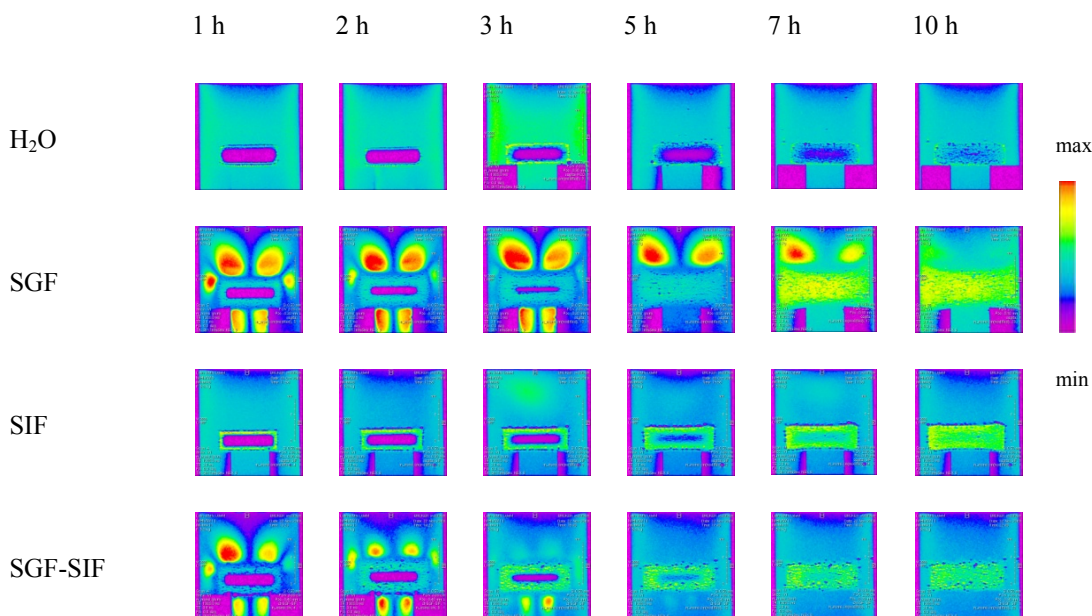

Figure 4.1. The NMR images of the CMS-chitosan complex tablets immersed in various media at 37 ^{o}C for 1, 2, 3, 5, 7 and 10 h. The bright spots above the tablets resulted from an abrupt change of magnetic susceptibility at the interface between the gel layer and the liquid. SGF-SIF indicates that the tablets were transferred from SGF to SIF after immersion for 2 h in SGF.

The proton density profiles shown in Figure 4.2 are taken from the NMR images of the samples and offer a clearer picture of magnitude of the water signal as a function of time. The profiles were plotted along the radial direction going through the center of the tablets. As

mentioned earlier, all the images are T_1-weighted due to the short repetition time. Water concentration in the gel layer is not strictly proportional to the proton density but the trend is correct inside a tablet.

4.4.2. Comparison of Polymer Matrices.

The NMR images and the proton density profiles show that the CHAS tablets swell at the slowest rate among the four matrices. The dry core of a CHAS tablet disappears after immersion in a medium for more than 7 hours. The hydrated tablet continues to swell very slowly until reaching equilibrium at more than 24 h. As expected, the swelling of the CHAS tablet shows little difference in the different external media used since the matrix is stabilized mainly by hydrogen bonding. Basket-shaped spin-density profiles with flat bottoms present the slow process of water penetration in a CHAS tablet. Low water signals have already been detected in the core after 2 hours, long before the polymer concentration becomes homogeneous in 10 hours. The signal intensity of the core gradually increases with time.

In contrast, water moves very fast in CMS and the water fronts meet inside a CMS tablet after immersion for only 3 hours. It appears (Figure 4.5) that the CMS tablets lack a well-defined edge owing to the similar proton density of the loose gel at the periphery. Since SGF has a pH lower than the pK_a (4.8) of CMS, the carboxyl groups are protonated and the resultant hydrogen bonds lead to a polymer network which restricts the movement or relaxation of the gel and keeps the integrity of the tablets. The swelling ratio in SGF is the lowest for the CMS tablets. These results fit well with previous observation of the shape and behavior of the CMS tablets.[5, 34, 35] In SIF and water with pH values higher than the pK_a of CMS, the carboxyl groups are ionized. Hydrogen bonds involving carboxylic groups were disrupted and an electrostatic repulsion occurred among polymer chains, allowing water to readily diffuse into the hydrogels. A higher swelling ratio was observed. A bump-shaped change in the proton density was observed in the hydrated outer layer when the gel is very loose, which is common for the CMS tablets in SIF and water (Figure 4.8). The water front moves the most slowly in the case of SGF. A sharp "peak" well defines the border of a tablet at 0.5 h. The slow rate to reach equilibrium for a CMS tablet in SIF and water shows that the anionic matrix may offer limited sustained drug release of drugs.

Chitosan dissolved in acidic SGF and a thick layer of transparent gel was formed very quickly around the hard core. The core decreases gradually with time while the matrix dissolves in the medium. Within 2 h the hydrogel already filled the NMR tube with a diameter of 18.2 mm. No proton signal was detected in the dry core until the core completely disappeared, as shown by the clear-cut feature of the proton density profile. The chitosan tablets rapidly disintegrated in both SIF and H_2O, and no NMR image could be acquired to allow any measurement of swelling ratio.
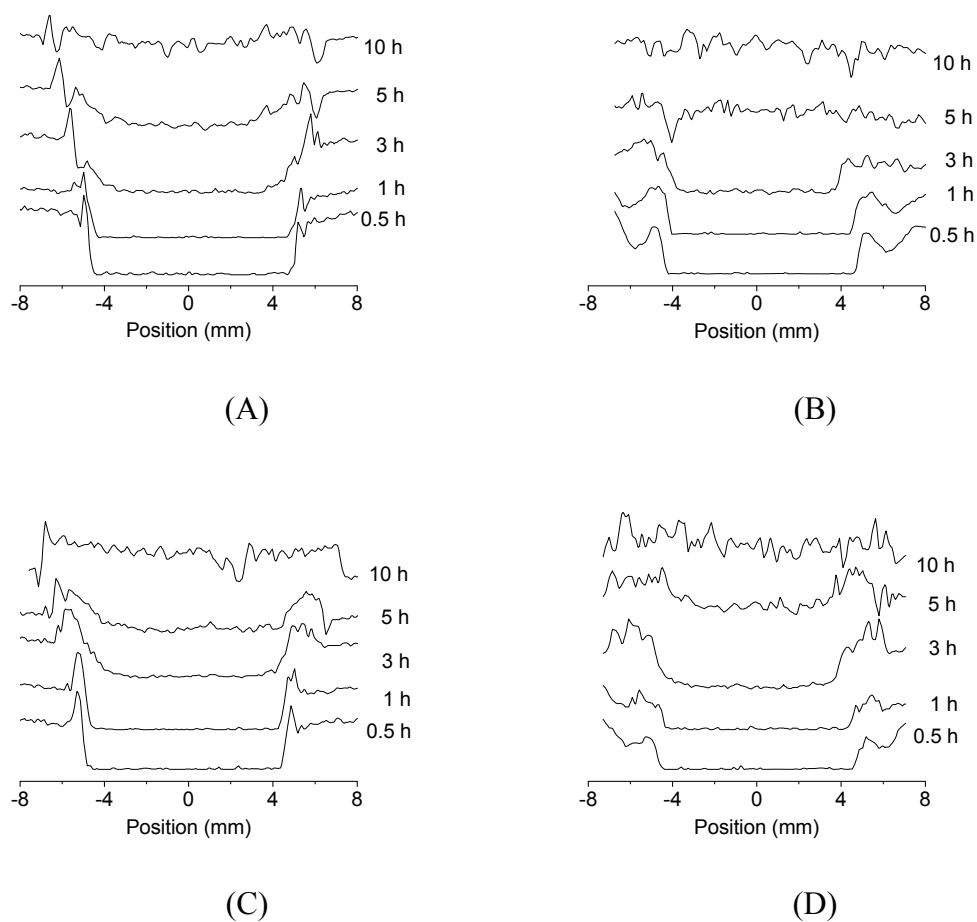

Figure 4.2. The change of the proton density profiles of the tablets made of the CMS-chitosan complex immersed in (A) H_2O, (B) SGF, (C) SIF, (D) SGF-SIF at 37 $^{\circ}$C at different immersion times.

A tablet made of CMS-chitosan complex presents swelling characteristics similar to those of CHAS, but with slightly faster swelling. The features are very different from those of

the individual components, CMS and chitosan. The interaction between CMS and chitosan retards the diffusion of water. The tablets of the complex swell much more slowly than those of CMS and chitosan. A gel layer was formed more rapidly in SGF than in other media and kept expanding until reaching the tube wall in 7 hours (Figure 4.1). The gel is mostly formed by chitosan which dissolves in SGF. At the same time, the dry core diminishes faster than in the other media. At the 5th hour, the proton density profile shows that the proton signal inside the tablets became uniform, while the tablets in the other media needed a few more hours to complete the process. When the fluid was changed from SGF to SIF, the volume of the gel layer either leveled off or decreased due to the still protonated chitosan having a strong interaction with ionized CMS.

The preparation procedure may help to explain the compact shape of the complex tablets in neutral media (H_2O and SIF) and their pronounced swelling in SGF. The chitosan solution (pH 3.6) was added to the CMS solution (pH 6.8) to prepare the complex. During the mixing process, the pH value became close to pK_a of chitosan (pH 5.2 − 6.8). The formation of the complex was due to the electrostatic interaction between NH_3^+ and COO^- and the hydrogen bonds between NH_2 and COOH groups. Since at pH 5 – 7 the majority of the amino groups of the chitosan were non-ionized while the carboxyl acid groups were ionized (deprotonated) when the precipitation took place, the complex formed by the two different types of polymer ionized polymer chains contained idle NH_2 groups (not involved in the interaction). In SGF (pH 1.2), most of the carboxylic acid groups and the amino groups were protonated, leading to the dissociation of the NH_3^+ and COO^- groups. The chitosan (non-associated) in the complex exhibited significant swelling. A similar chitosan-based complex with pectin was reported[36] prepared at pH 5.0 at mixing molar ratios (pectin:chitosan) of 9:1, 7:3, and 1:1. The swelling of the complex of chitosan (pK_a 6.3) and pectin (pK_a 4.0) showed significant pH dependence when the molar ratio is high. The pH effect was substantially reduced when the molar ratio decreased.

4.4.3. Swelling Characteristics of the Tablets

The radial and axial swelling data extracted from the images at different immersion times (Figure 4.3) provide quantitative information of the change in shape and dimension of the tablets. In the case of SGF-SIF treatment, when tablets are switched to SIF at 2 h, a sudden

change occurs and the swelling curve is approaching the curve of SIF. This behavior is most obvious in the case of the complex tablets (Figure 4.3 E-F).
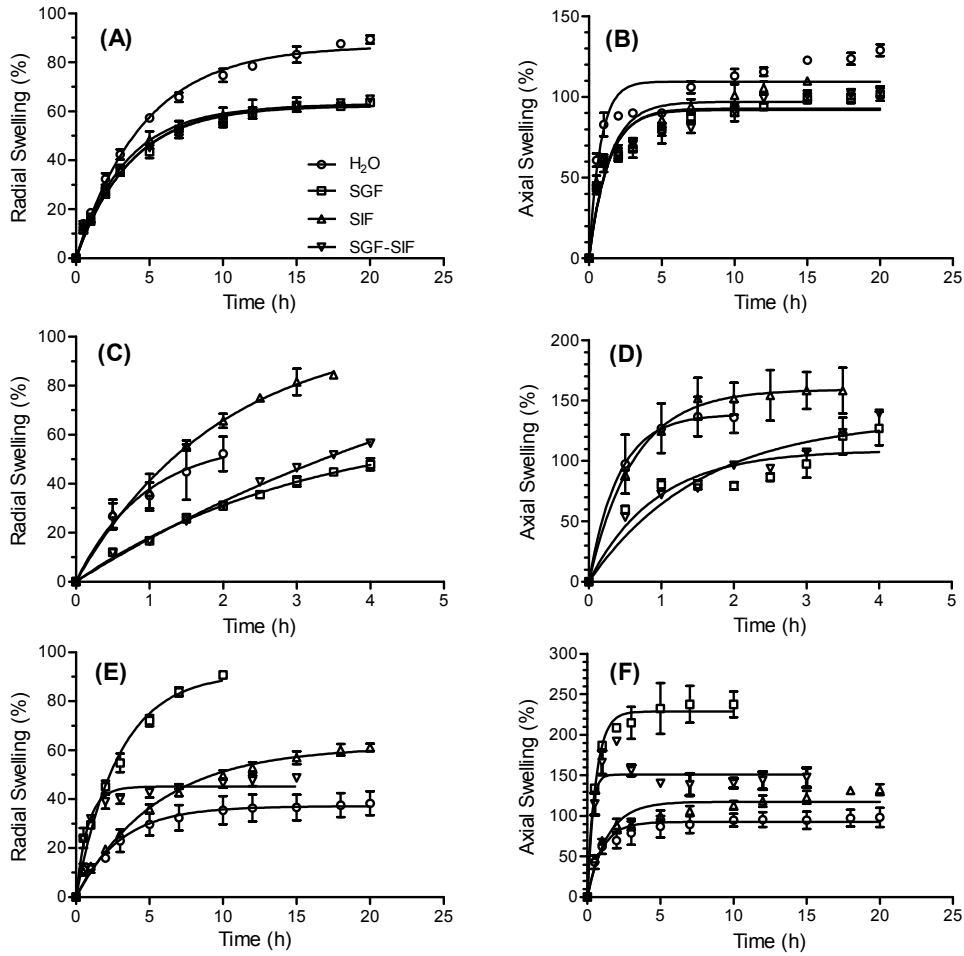

Figure 4.3. The radial and axial swelling of the CHAS tablets (A and B), of the CMS tablets (C and D), and of the complex tablets (E and F) in H_2O, SGF, SIF, and SGF-SIF. Lines are fits to Eq. 2.

The percentage of the swelling of the tablets is defined by

$$S = \frac{d - d_0}{d_0} \times 100\% \qquad (4.1)$$

where S is the percentage of swelling and d and d_0 are the dimensions (thickness or diameter) of the tablet at immersion time t and at the beginning, respectively. The swelling data can be fitted to

$$S = S_{\max}(1 - \exp(-k_s t))$$ (4.2)

where $S_{\max}$ is the swelling at equilibrium and k_s the rate constant of the swelling process.

Table 4.1. Swelling of the tablets made of CHAS, CMS, CMS-chitosan complex. Parameters obtained by fitting to Eq. 4.2. The measurements were carried out on triplicates; the reported values are the averages and the uncertainties correspond to the standard deviations.

media	radial dimension			axial dimension		
	$S_{\max}$ (%)	k_s (10^{-5}s^{-1})	R^2	$S_{\max}$ (%)	k_s (10^{-4}s^{-1})	R^2
CHAS						
H$_2$O	86.8±1.1	6.1±0.2	0.992	109±3	3.6±0.5	0.877
SGF	62.2±0.7	7.5±0.3	0.989	91.8±2.1	2.2±0.2	0.894
SIF	62.2±1.2	8.2±0.4	0.985	96.9±3.1	2.0±0.3	0.886
SGF-SIF	63.0±0.7	7.4±0.3	0.990	92.7±2.3	2.1±0.3	0.878
CMS						
H$_2$O	57±8	30±9	0.903	139±7	6.8±1.5	0.932
SGF	66.6±3.8	8.8±0.8	0.991	109±6	3.0±0.6	0.841
SIF	103±7	14.2±1.8	0.982	159±4	4.5±0.5	0.963
SGF-SIF	128±24	4.1±1.0	0.996	135±14	1.8±0.5	0.937
CHAS-CMS Complex						
H$_2$O	37.1±1.2	9.2±1.1	0.907	92.6±2.1	2.8±0.4	0.890
SGF	91.4±2.8	9.6±0.8	0.976	229±4	4.6±0.4	0.959
SIF	61.4±1.1	5.0±0.2	0.987	117±3	2.0±0.2	0.911
SGF-SIF	45.1±0.7	34.9±2.6	0.966	151±4	9.4±2.0	0.883

For all the tablets, the axial swelling was much higher than the radial swelling, and the rate constant along axial direction is an order of magnitude higher (Table 4.1). As expected, the CHAS tablets did not show any pH effect, but ionic strength influenced the swelling. Thus, the dimensions of the swollen tablets in both SGF and SIF are smaller than those in distilled water (65 vs. 90% radially and 100 vs. 130% axially). An increase in the ionic strength causes a decrease in the osmotic pressures (due to hydration of ionic species), leading to a reduction of swelling. For the other three matrices, i.e, CMS, chitosan and the complex, the effect of pH was more significant than that of ionic strength (Figure 4.3 C-F).

The swelling of the CMS tablets was lower in SGF than in neutral media due to the protonation of the COOH groups. In SGF-SIF, the tablets swelled to a similar extent as in SGF. Differently, the swelling of the complex tablets in SGF was almost twice of those in other media (Table 4.1). The tablets in distilled water had the solid-like appearance due to a very slow swelling process. The outer gel layer of CMS-chitosan tablets was thicker than that of a CMS tablet, but water diffusion was slower in its core (Figure 4.1). According to the swelling characteristics, drug could be released in a controlled way by the complex after an initial burst dissolution of the drug located near the surface of a tablet.

The *in vitro* dissolution experiments of monolithic tablets made of the complex loaded with 20 wt% aspirin showed a sustained release up to 30 hours, longer than expected.[30] By contrast, 90% of the loaded aspirin was released in about 11 hours when CMS or chitosan alone was used as the excipient.[30] Aspirin has a water solubility of 4.6 mg/mL[37] and its pK_a is 3.5. The relatively long sustained drug release of aspirin from the complex tablets can be a result of a binding interaction with either CMS or chitosan in acidic and neutral media, respectively. During the first two hours in SGF, the hydrogen bonding among the carboxyl acid groups of aspirin and CMS slowed down the drug release. In SIF, the interaction between aspirin and chitosan may become more predominant than the hydrogen bonding in the system, reducing the diffusion rate of aspirin out of the hydrated membrane of the matrix. In the case of acetaminophen,[30] a drug with slightly higher water solubility (14 mg/mL)[37] and with higher pK_a (9.4), the best release was afforded by chitosan excipient alone due to a possible interaction between acetaminophen and chitosan in the physiological media. The CHAS tablets showed a similar release profile of acetaminophen to those of complex.[26, 30]

4.5. Conclusion

Both CMS and chitosan have demonstrated pH-dependent swelling capabilities. The tablets made of the complex of CMS and chitosan presented a combined benefit of a lower swelling in acidic media than those of chitosan alone and a slower water uptake than CMS in neutral media. A considerable decrease in swelling (60% radially and 150% axially) in neutral media is observed by NMRI for the complex tablets in comparison with those of CMS and chitosan. Similar to CHAS, the complex tablets can keep their integrity after the tablet swelling reaches an equilibrium. The interaction between the carboxyl groups of CMS and

amine groups of chitosan showed a similar stabilizing effect as hydrogen bonding in the case of covalent cross-linked starch. The *in-vitro* dissolution experiments presented a particularly slow release of aspirin from the monolithic tablets with 20 wt% drug loading.[30] The results showed that the complex of CMS and chitosan is a promising polymer excipient for sustained drug release, by partially retaining the gastroprotective effect of CMS and by modulating its solubility in neutral media through ionic association with chitosan. This behaviour makes the novel complex a good excipient to colon delivery. Its swelling properties may be modulated by pH and ionic strength of the processing medium and the molar ratio of the two components.

4.6. Acknowledgements
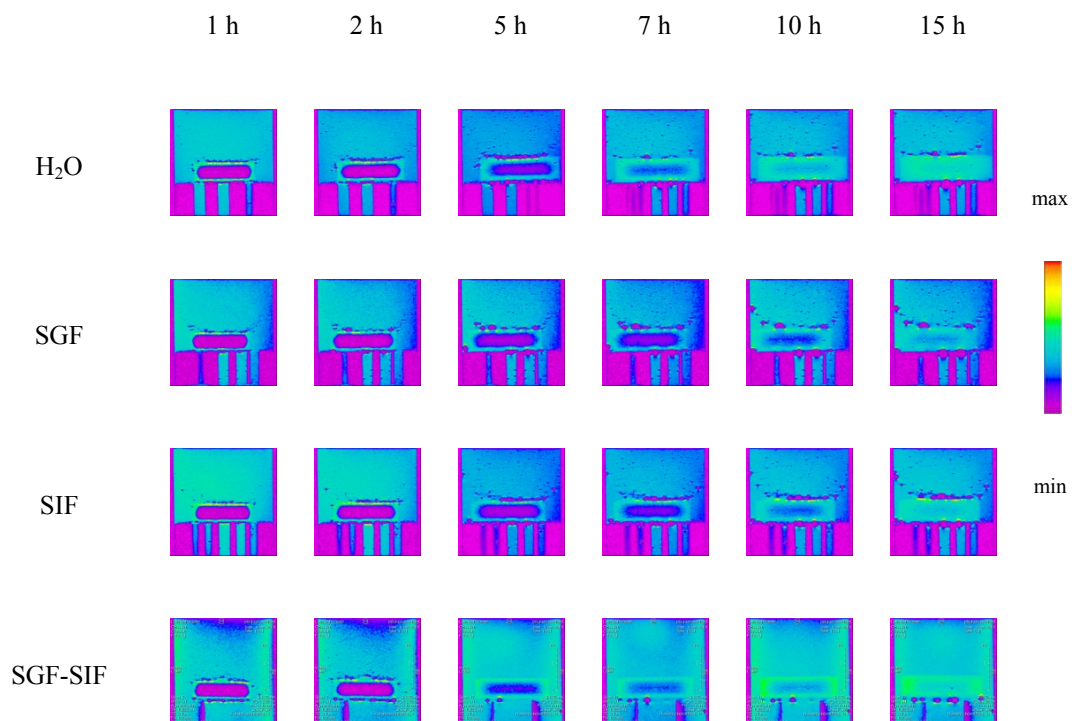
4.7. Supporting Information

Figure 4.4. The NMR images of the CHAS tablets immersed in various media at 37°C for 1, 2, 5, 7, 10 and 15 h. The part at the bottom of the images is the Teflon support. The dark spots around the tablets are air bubbles.
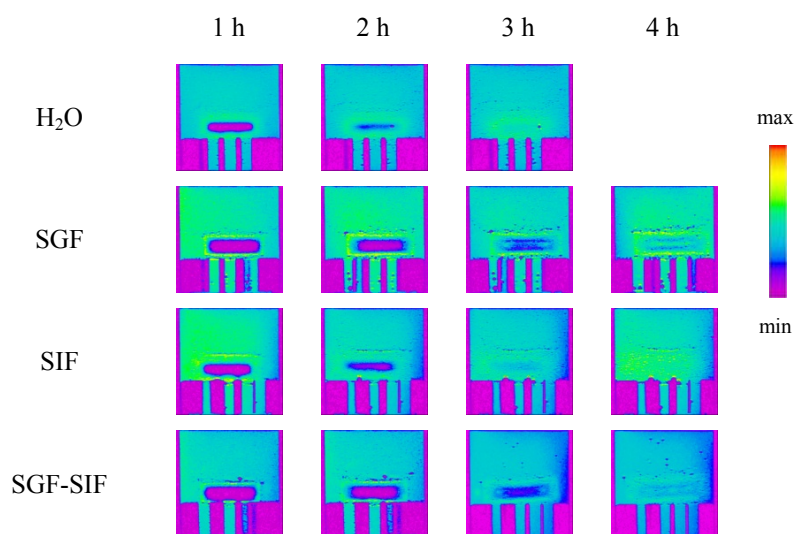

Figure 4.5. The NMR images of the CMS tablets immersed in various media at 37 °C for 1, 2, 3 and 4 h.
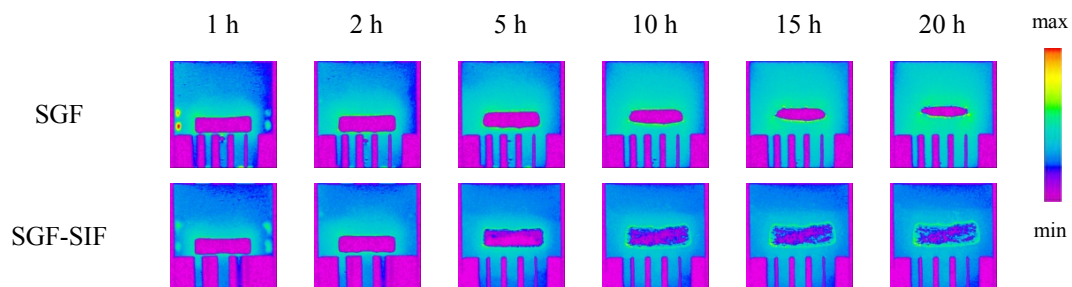
Figure 4.6. The NMR images of the chitosan tablets immersed in various media at 37 $^{\circ}$C for 1, 2, 5, 10, 15 and 20 h.

Figure 4.7. The change of the proton density profile of the CHAS tablets immersed in (A) H_2O, (B) SGF, (C) SIF and (D) SGF-SIF at 37 $^{\circ}$C.
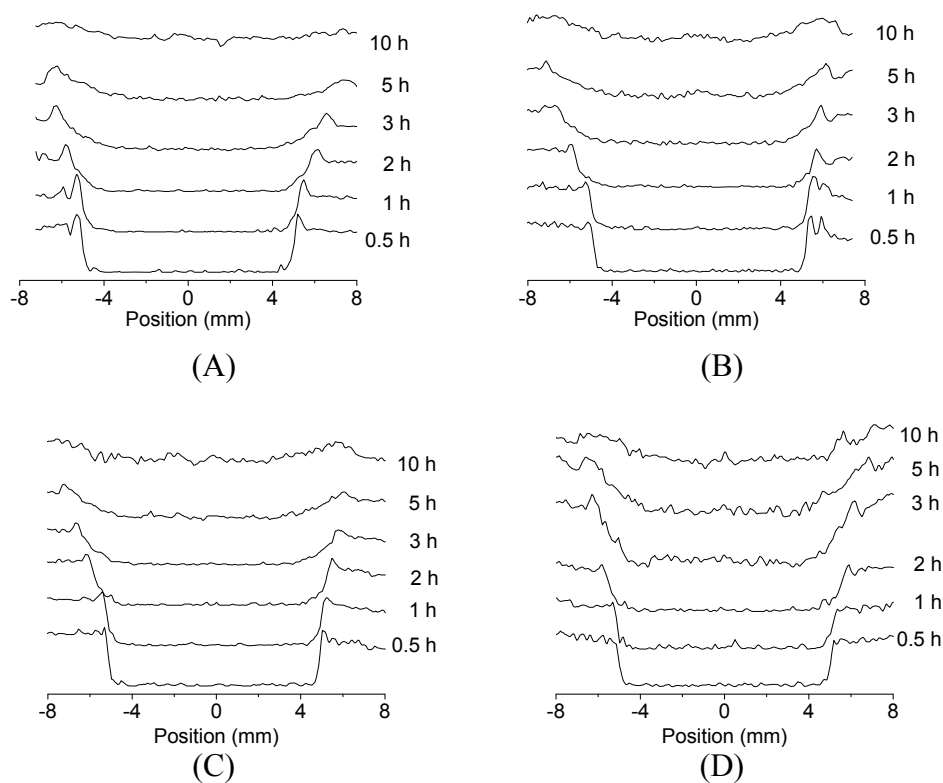
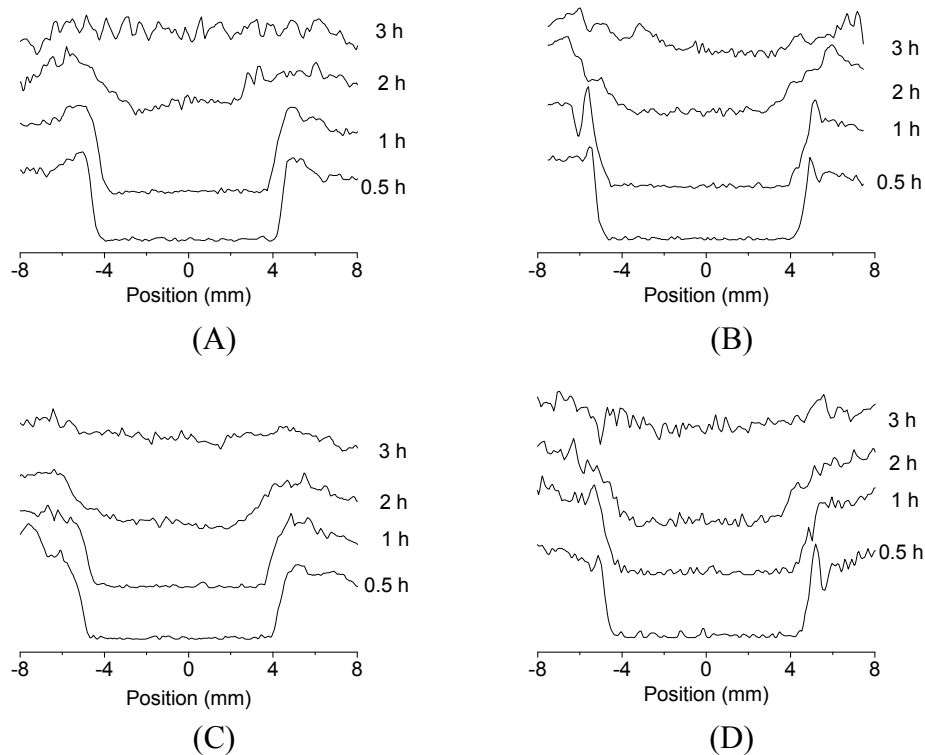**Figure 4.8.** The change of the proton density profile of the CMS tablets immersed in (A) H_2O, (B) SGF, (C) SIF and (D) SGF-SIF at 37 ^{o}C.
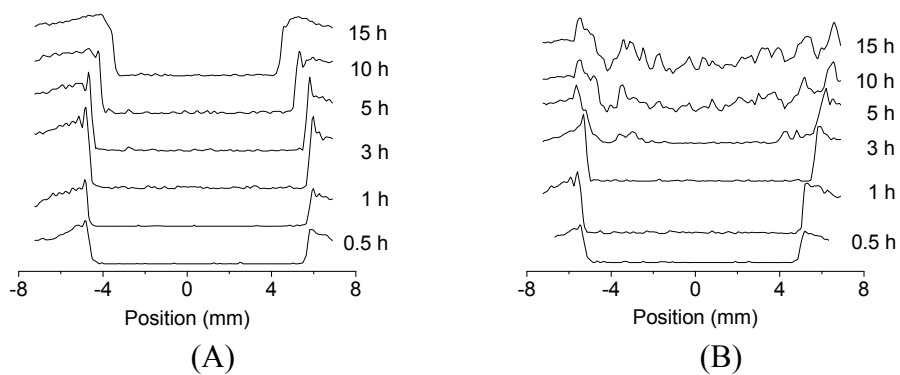

Figure 4.9. The change of the proton density profile of the chitosan tablets immersed in (A) SGF and (B) SGF-SIF at 37 ^{o}C.
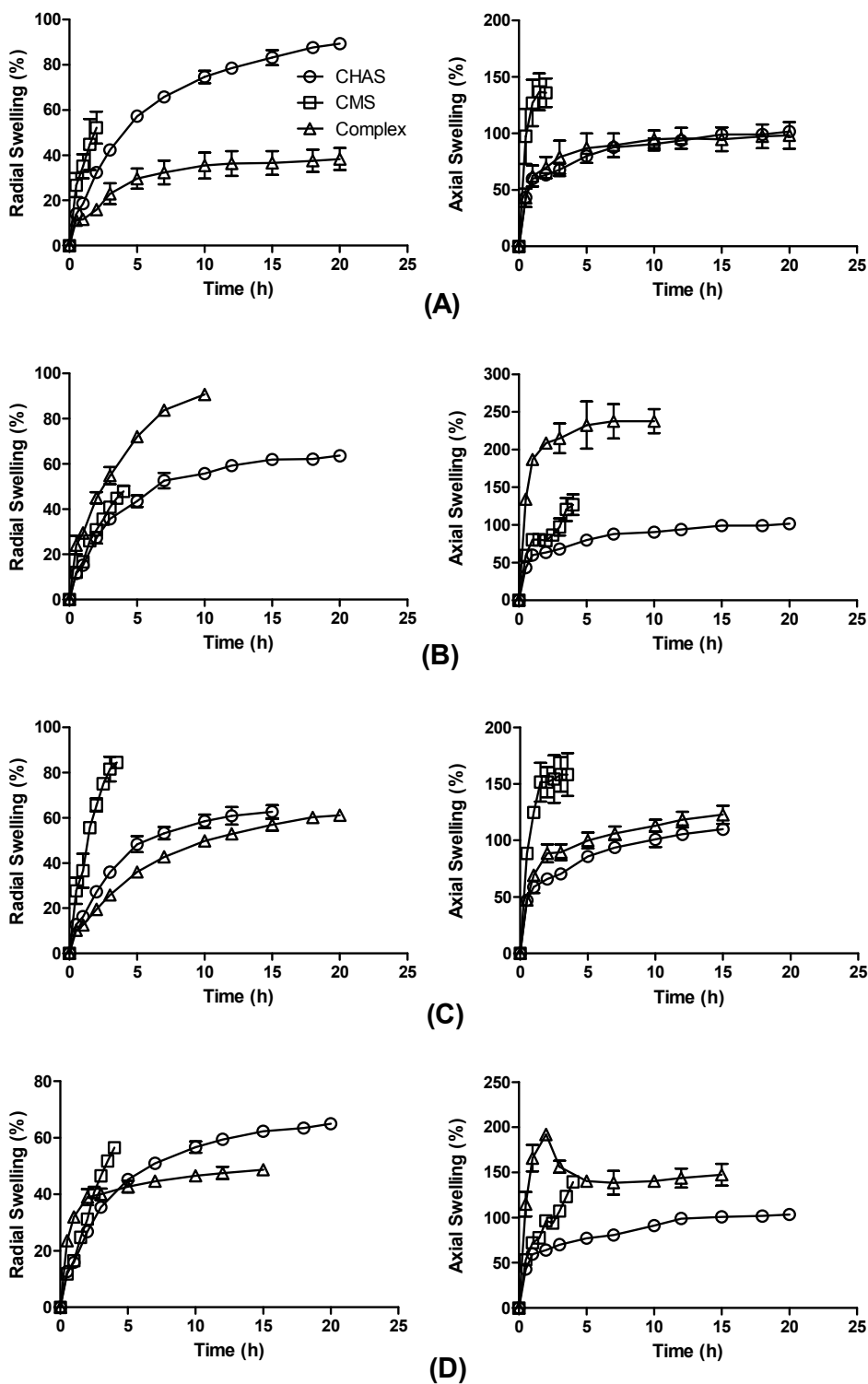
Figure 4.10. The radial and axial swelling of the CHAS, CMS and CMS-chitosan complex tablets in (A) H$_2$O, (B) SGF, (C) SIF and (D) SGF-SIF.

4.8. References

1. Jain, K. K., *Drug Delivery Systems*. Humana Press: Totowa, NJ, 2008; p 220-224.

2. Dumoulin, Y.; Alex, S.; Szabo, P.; Cartilier, L.; Mateescu, M. A. *Carbohydr. Polym.* **1998,** 37, 361-370.

3. Wong, D. W. S., *Mechanism and Theory in Food Chemistry*. Springer: New York, 1989.

4. Lammers, G.; Stamhuis, E. J.; Beenackers, A. A. C. M. *Ind. Eng. Chem. Res.* **1993,** 32, 835-842.

5. Assaad, E.; Mateescu, M. A. *Int. J. Pharm.* **2010,** 394, 75–84.

6. Sen, G.; Pal, S. *J. Appl. Polym. Sci.* **2009,** 114, 2798-2805.

7. Mulhbacher, J.; Ispas-Szabo, P.; Mateescu, M. A. *Int. J. Pharm.* **2004,** 278, 231-238.

8. Calinescu, C.; Nadeau, E.; Mulhbacher, J.; Fairbrother, J. M.; Mateescu, M. A. *Int. J. Pharm.* **2007,** 343, 18-25.

9. Rathbone, M. J., *Modified-Release Drug Delivery Technology*. Informa Healthcare: New York, 2008; Vol. 2.

10. Calinescu, C.; Mateescu, M. A. *Eur. J. Pharm. Biopharm.* **2008,** 70, 582-589.

11. Kumar, M. N. V. R.; Muzzarelli, R. A. A.; Muzzarelli, C.; Sashiwa, H.; Domb, A. J. *Chem. Rev.* **2004,** 104, 6017-6084.

12. Kaur, G.; Rana, V.; Jain, S.; Tiwary, A. K. *AAPS Pharm. Sci. Tech.* **2010,** 11, 36-45.

13. Park, S.-H.; Chun, M.-K.; Choi, H.-K. *Int. J. Pharm.* **2008,** 347, 39-44.

14. Zhang, Y.; Shi, B.; Li, C.; Wang, Y.; Chen, Y.; Zhang, W.; Luo, T.; Cheng, X. *J. Control. Release* **2009,** 136, 172-178.

15. Mao, H.-Q.; Roy, K.; Troung-Le, V. L.; Janes, K. A.; Lin, K. Y.; Wang, Y.; August, J. T.; Leong, K. W. *J. Control. Release* **2001,** 70, 399-421.

16. Bhattarai, N.; Gunn, J.; Zhang, M. *Adv. Drug Deliv. Rev.* **2010,** 62, 83-99.

17. Berger, J.; Reist, M.; Mayer, J. M.; Felt, O.; Gurny, R. *Eur. J. Pharm. Biopharm.* **2004,** 57, 35–52.

18. Swarbrick, J., *Encyclopedia of Pharmaceutical Technology*. 3rd ed.; Informa Healthcare: New York, 2006.

19. Richardson, J. C.; Bowtell, R. W.; Mader, K.; Melia, C. D. *Adv. Drug Deliv. Rev.* **2005,** 57, 1191-1209.

20. Djemai, A.; Sinka, I. C. *Int. J. Pharm.* **2006,** 319, 55-62.

21. Baumgartner, S.; Lahajnar, G.; Sepe, A.; Kristl, J. *Eur. J. Pharm. Biopharm.* **2005,** 59, 299-306.

22. Baille, W. E.; Malveau, C.; Zhu, X. X.; Marchessault, R. H. *Biomacromolecules* **2002,** 3, 214-218.

23. Malveau, C.; Baille, W. E.; Zhu, X. X.; Marchessault, R. H. *Biomacromolecules* **2002,** 3, 1249-1254.

24. Thérien-Aubin, H.; Baille, W. E.; Zhu, X. X.; Marchessault, R. H. *Biomacromolecules* **2005,** 6, 3367-3372.

25. Thérien-Aubin, H.; Zhu, X. X.; Ravenelle, F.; Marchessault, R. H. *Biomacromolecules* **2008,** 9, 1248-1254.

26. Wang, Y. J.; Ravenelle, F.; Zhu, X. X. *Can. J. Chem.* **2010,** 88, 202-207.

27. Fyfe, C. A.; Blazek, A. I. *Macromolecules* **1997,** 30, 6230-6237.

28. Thérien-Aubin, H.; Zhu, X. X. *Carbohydr. Polym.* **2009,** 75, 369-379.

29. Mulhbacher, J.; Ispas-Szabo, P.; Lenaerts, V.; Mateescu, M. A. *J. Control. Release* **2001,** 76, 51-58.

30. Assaad, E.; Wang, Y. J.; Zhu, X. X.; Mateescu, M. A. *Carbohydr. Polym.*, accepted.

31. US Pharmacopeia National Formulary U.S.P. XXIV, 2000. In United States Pharmacopeial Convention Inc.: Rockville, MD.

32. Bock, C.; Frederich, M.; Wittig, R.-M.; Pörtner, H.-O. *Magn. Reson. Imaging* **2001,** 19, 1113–1124.

33. Bock, C.; Sartoris, F.-J.; Pörtner, H.-O. *Magn. Reson. Imaging* **2002,** 20, 165–172.

34. Calinescu, C.; Mulhbacher, J.; Nadeau, T.; Fairbrother, J. M.; Mateescu, M. A. *Eur. J. Pharm. Biopharm.* **2005,** 60, 53-60.

35. Lemieux, M.; Gosselin, P.; Mateescu, M. A. *AAPS Pharm. Sci. Tech.* **2010,** 11, 775-785.

36. Bigucci, F.; Luppi, B.; Cerchiara, T.; Sorrenti, M.; Bettinetti, G.; Rodriguez, L.; Zecchi, V. *Eur. J. Pharm. Sci.* **2008,** 2008, 435-441.

37. DrugBank: a knowledgebase for drugs, drug actions and drug targets. . http://www.drugbank.ca/ (Oct. 8, 2010)

5. Conclusion

Molecular diffusion in hydrogels has been a subject of great importance with respect to both fundamental research and practical applications of polymers used for biomedical and pharmaceutical applications. Two related NMR techniques, PGSE NMR spectroscopy and NMR imaging, have been used to study the characteristics of controlled drug-delivery systems based on polymers including PVA, CHAS, CMS, chitosan and CMS-chitosan complex. The diffusion properties of small molecules and macromolecules in aqueous solutions and gels have been studied and compared.

5.1. The diffusion of Star Polymers in PVA Solutions and Gels

PGSE NMR spectroscopy has been used to study the diffusion of star-shaped polymers in polymer solutions and gels. This technique can be applied easily to measure the self-diffusion coefficients of small and large molecules in polymer solutions and gels, especially for certain diffusant probes inaccessible to other techniques, such as fluorescence photobleaching recovery, confocal fluorescence microscopy and dynamic light scattering. It is a rapid and noninvasive method and requires only a small amount of the sample. The results can also provide the hydrodynamic radii (R_H) of the diffusants, which are related to the structure of the molecules. The model of Petit et al. developed in our group also provides a comparison of the jump frequencies of different probes in the same polymer gel.

The experiment is sensitive to thermal convection currents in the sample, so a precise temperature control is needed. If the probe molecules have overlapping resonances, they could be separated based on the differences among their diffusion coefficients on a 2D spectrum (with chemical shift on one axis and the distribution of diffusion coefficients on the other axis). But the data processing is much more time-consuming and strongly depends on the method and the input data.

The diffusion of the star-shaped polymers with a cholic acid core and four PEG arms were studied. Their diffusion in aqueous solutions and PVA gels were compared with those of other PEG-based macromolecules of linear and dendritic architectures. The results showed that the star polymers have an intermediate diffusion rate between the dendrimers and the linear PEGs of comparable molecular weight. The diffusion rate is essentially dominated by the density of the molecules, which has been shown by the comparisons between linear and cyclic PEGs.

T_1 measurements of different moieties of the star-shaped polymers were used to determine their conformations in the solutions and the change in mobility with increasing concentration. The four PEG arms have a higher mobility than the cholic acid core of the star polymers, indicating the star polymers have a similar conformation as the PEG-based dendrimers.

5.2. The Study of the Effect of Drug Loading

NMRI has been used to study selected tablets for controlled drug delivery systems. NMRI is a noninvasive and effective method to record the dynamic change of the tablets. NMRI typically observes the mobile ^{1}H associated with free water, whereas the fast decaying ^{1}H nuclei associated with polymer network and bound water are mostly invisible due to their short T_2 values. The dimensional change of a tablet immersed in a medium is given by the images acquired at predefined intervals. By integration of the proton intensity profiles, the liquid uptake may be obtained, which gives more accurate results than the commonly-used weighing method. Moreover, diffusion-weighted imaging provides diffusion coefficients explicitly, which can be used to probe the microscopic spatial heterogeneity of a polymer network.

The effect of drug loading on the swelling was studied with the CHAS tablets loaded with different amounts of acetaminophen (10, 20 and 40 wt%). The study showed that the presence of drug molecules accelerated water uptake due to the changes in the chemical potential gradient. The higher drug loading led to faster water diffusion into the tablet. The

drug solubility and the degree of drug loading have little influence on the diffusion coefficient of water in the outer membrane formed at the interface of the bulk water and the tablets. Inside the tablets, water diffuses faster for tablets with higher drug loading and increases gradually with time.

Despite the different rates of water uptake and diffusion in the tablets, the percentage of the drug released remained similar for all the CHAS tablets. The outer membrane ensured a controlled release of acetaminophen, regardless of the amount of drug in the tablet.

The changes of the water diffusion coefficient and the tablet swelling strongly depend on the solubility of the drug and the loading level. The drug releasing rate merely undergoes a minor change with increasing drug loading amount. Compared to the CHAS tablets with no drug loaded, the tablets of 10 – 40 wt % acetaminophen swell substantially faster. The matrix is able to keep the integrity of all the tablets after their immersion in water for long time.

5.3. The Study of Various Polymer Matrices

The swelling of the CHAS tablets were compared with the tablets made of polyelectrolyte matrices including chitosan, CMS and CMS-chitosan complex in both acidic and neutral media. Simulated physiological liquids (SGF and SIF) were used for the *in vitro* study of the swelling and drug dissolution of the tablets. In the case of SGF, some artifacts appeared on the NMR images due to the relatively high ionic strength of SGF.

The tablets made of chitosan, CMS, and the CMS-chitosan complex showed pH-sensitive swelling due to the presence of $-COONa$ and/or $-NH_2$ functional groups. The CMS-chitosan complex tablets have similar swellings to those of CHAS tablets in neutral media. But the complex tablets in SGF showed a greater extent of swelling. The remarkable dimensional change in SGF is mainly contributed by chitosan that is dissociated from CMS.

The effect of pH is more pronounced than that of the ionic strength for the tablets without drug loading. The swelling in various pH depends on the pK_a of the matrix. In the case of drug-loaded tablets, the drug release rate is affected by the pK_a values of both the matrix and the drug rather than the drug loading level.

5.4. Future Work

5.4.1. Research Techniques

In the NMRI studies of polymer matrices, a more precise definition of the penetration front may be useful. The front is currently defined by proton density profiles taken from the NMR images. However, very low water content may not be detectable by NMRI due to their short spin-spin relaxation times (T_2). This may be improved by T_2 imaging of the tablets combined with 1D imaging. In addition, a theoretical NMR signal intensity profile may be obtained when T_1 and T_2 have been measured. The use of theoretical rather than the apparent NMR signal intensity also make the definition of the glassy core more precise, which can be compared with the experimental determination of swelling and penetration fronts.

A NMRI coupled with a dissolution system may be built to acquire images while drug release is measured simultaneously. A study of tablet dissolution and the subsequent drug release would be useful if the study is carried out under controlled conditions with flow or another form of agitation. A common practice is to incorporate a flow-through cell inside the bore of the magnet. UV-vis spectroscopy or HPLC may be employed to measure the total drug release.

5.4.2. Choice of Diffusing Probes

A series of hydrophilic PEG star polymers without a hydrophobic core may be studied in terms of their diffusion properties in aqueous solutions and PVA gels. By comparing these diffusants with those having been studied, including the linear, dendritic PEGs and the star polymers with a cholic acid core, the effect of the core on the diffusion of the polymeric probes may be better elucidated, leading to a better understanding of the effect of polymer architecture.

Complexation between oppositely charged polyelectrolytes proved to be a promising method to prepare microspheres for drug delivery applications. However, the dissociation of the anionic and cationic polymers in gastric media might occur due to the reversibility of the cross-linking by electrostatic interactions, which usually causes an undesired fast release of the loaded drug in the stomach. In the case of the chitosan complexes, the rate of the swelling and erosion of the tablets in SGF has been reduced with respect to chitosan itself, but the

complex showed little effect on slowing down the release in SGF. An accurate control of the complex preparation process, such as pH, ionic strength of the media, order of mixing of the components may modify the complex formulation in the acidic environment. The second route to improve the performance of the complex in SGF is to prepare the complex of CMS and chitosan with increased negative charge density.

5.4.3. Choice of Drugs

The release of the drugs with low and intermediate solubilities (ciprofloxacin and acetaminophen) has been studied in the solid dosage forms of CHAS. The limited swelling and compact feature of the CHAS tablets showed a strong capacity to control the release of those drugs. Other drugs with higher solubilities could be tested to check the upper loading limit of the CHAS tablets. These drugs may include amoxicillin trihydrate (solubility ca. 3500 mg/L) and the highly soluble metformin.

The release of the drugs of intermediate and high solubilities (aspirin, acetaminophen and metformin) has been studied with the chitosan-CMS complex as the carrier. The complex tablets with acetaminophen (pK_a 9.4) loaded had 80% of drug released within 7 hours (chapter 4). In the case of aspirin (pK_a 3.5), however, the duration was significantly prolonged to over 20 hours (chapter 4). Although the drug release is difficult to control in gastric fluid by the chitosan-CMS complex, a drug insoluble in acidic media, such as diclofenac (solubility ca. 50 mg/mL, pK_a 4.15), may benefit from the formulation. Diclofenac bears a carboxyl acid group which may interact with dissociated chitosan in the solution of low pH, probably causing a delayed release.

Appendix

Pharmaceutical Polysaccharides: Pectin, Alginate, and Carrageenan

Pectin, an anionic polysaccharide, is extracted from citrus fruit and apple pomace. It consists primarily of chains of galacturonic acid units (which can be randomly acetylated and methylated) linked as 1,4-α-glucosides (Figure A1). It is soluble in water.
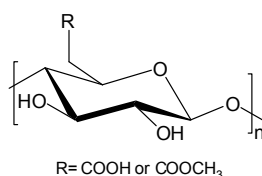

R= COOH or COOCH$_3$

Figure A1. The chemical structure of pectin.

Chitosan can act as an effective crosslinker of pectin networks under slightly acidic conditions. Gelation behaviour is dependent on the degree of esterification of the pectin and concentration of the crosslinker.[1] Zero-order kinetics was achieved using a binary polymer matrix consisting of highly methoxylated pectin and HPMC at different ratios (4:5, 3:6, and 2:7), both in the case of soluble and poorly soluble drugs, as a result of rapid hydration/gelation in both axial and radial directions.[2]

Widely used in food industry as a gelling agent and a stabilizer, pectin has been approved by USFDA as an inactive ingredient in oral tablets and capsules.[3]

Alginates are polysaccharide polymers isolated from brown seaweed. Alginate (Figure A2) is a linear copolymer composed of 2 monomeric units, D-mannuronic acid (M) and L-guluronic acid (G). The monomers can appear in homopolymeric blocks of consecutive G-residues, consecutive M-residues, alternating M and G-residues, or randomly organized blocks. The pK$_a$ values for mannuronic and guluronic acid monomers are 3.38 and 3.65, respectively.[4]
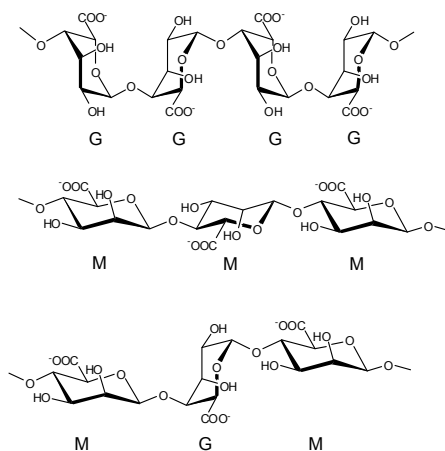
Figure A2. The chemical structures of G and M blocks of alginate.

Monovalent metal ions form soluble salts with alginate whereas divalent and multivalent cations (except Mg^{2+}) form gels or precipitates. The calcium alginate gels have been extensively studied. The fast drug release of Ca^{2+}-alginate based systems can be improved by modifying the microsphere surface using polycations (chitosan/poly-L-lysine).[5] Alginate may form an acid gel and an ionotropic gel dependent on pH. The physicochemical properties of the polymer system and the swelling process are dependent on the type of gel formed.[6] Alginate-chitosan-based drug delivery systems provide a striking improvement in the pharmacokinetic parameters.[7] The preparation of alginate-chitosan microspheres involves the cation-induced gelation of alginate, useful for the simultaneous encapsulation of the drug.

Ammonium calcium alginate, propylene glycol alginate, and sodium alginate have been approved by USFDA for using as inactive ingredients in oral tablets and capsules.[3]

Carrageenan is an anionic polysaccharide which is extracted from red seaweed. It consists of potassium, sodium, calcium, magnesium, and ammonium sulfate esters of galactose and 3,6-anhydrogalactose copolymers. It is soluble in water at 80°C. The carrageenans are divided into three families (κ-, ι-, and λ-carrageenan) according to the position of sulfate groups and the presence or absence of anhydrogalactose (Figure A3). The gelling ability becomes weaker in the order of κ-, ι-, and λ-carrageenan which possesses one, two, and three sulfate groups, respectively. Tablets based on carrageenan exhibit sensitivity to the pH and ionic strength of the media.[8] A study showed that the chitosan-alginate mixture could form hydrogel without disrupting the microstructure due to the high elastic modulus of

the swollen tablet, while tablets prepared from the chitosan-carrageenan mixture underwent a fast water uptake and a severe erosion process, leading to a less controlled drug release in acidic media (pH 1.2).[4] The difference was caused by the formation of polyelectrolyte complex due to the electrostatic bond between amino groups of chitosan and sulfonate groups of carrageenan. The interaction can only occur at pH values in the vicinity of the pK_a interval of the two polymers.[4] Alginate is un-ionized at pH 1.2 and thus no complexation can occur between alginate and chitosan.

Carrageenan, calcium carrageenan, and sodium carrageenan have been approved by USFDA for using as inactive ingredients in oral tablets and capsules.[3]
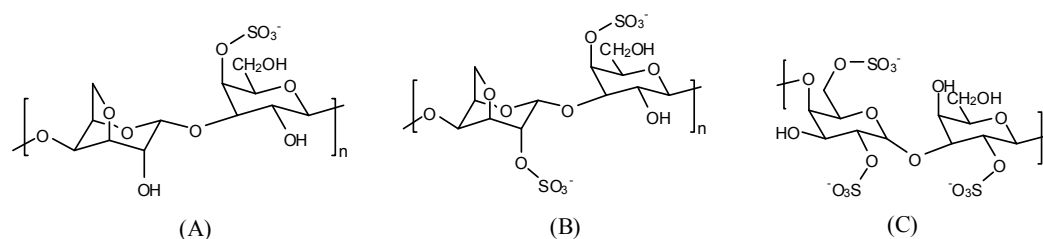

Figure A3. The chemical structures of (A) κ-carrageenan, (B) ι-carrageenan, and (C) λ-carrageenan

References:

1. Marudova, M.; MacDougall, A. J.; Ring, S. G. *Carbohydr. Res.* **2004,** 339, 1933-1939.
2. Kim, H.; Fassihi, R. *J. Pharm. Sci.* **1996,** 86, 316-322.
3. Inactive ingredients database. http://www.accessdata.fda.gov/scripts/cder/iig/index.cfm (April 3, 2010)
4. Tapia, C.; Corbaln, V.; Costa, E.; Gai, M. N.; Yazdani-Pedram, M. *Biomacromolecules* **2005,** 6, 2389-2395.
5. Ahmad, Z.; Khuller, G. *Expert Opin. Drug Deliv.* **2008,** 5, 1323-1334.
6. Tønnesen, H. H.; Karlsen, J. *Drug Dev. Ind. Pharm.* **2002,** 28, 621-630.
7. Khuller, R. P. K. *J. Antimicrob. Chemoth.* **2004,** 53, 635-640.
8. Gupta, V. K.; Hariharan, M.; Wheatley, T. A.; Price, J. C. *Eur. J. Pharm. Biopharm.* **2001,** 51, 241-248.